Spring 1978

The Photosynthetic Action Spectra of the Phytoplankton and Their Role in Governing Spatial and Temporal Distribution: A Numerical Modeling Approach

William Morrow Willis
Old Dominion University

THE PHOTOSYNTHETIC ACTION SPECTRA OF THE PHYTOPLANKTON AND THEIR ROLE IN GOVERNING SPATIAL AND TEMPORAL DISTRIBUTION: A NUMERICAL MODELING APPROACH

by

William Morrow Willis
B.S. June 1967, College of William and Mary, Virginia
M.S. August 1973, Old Dominion University, Virginia

A Dissertation Submitted to the Faculty of
Old Dominion University in Partial Fulfillment of the
Requirements for the Degree of

DOCTOR OF PHILOSOPHY

OCEANOGRAPHY

OLD DOMINION UNIVERSITY
May, 1978

Approved by:

Harris H. White (Director)

Chester E. Grosch

Anthony J. Provenzano

Frank P. Day

George S. Ofelt

John C. Ludwick

Abstract

In the present study a numerical modeling approach is employed to examine the role of division spedific differences in photosynthetic action spectra in governing the relative size of diatom and dinoflagellate carbon synthesis along various marine light regime gradients. A radiative transfer model taking into account both Rayleigh and Mie atmospheric optical properties is employed to define the light regime incident on the sea surface. The hydrospheric light regime is defined by an exponential decay model with a correction for diffuse back scatter. Taken together, the atmospheric and hydrospheric models define the spectral composition and intensity of light in the sea as a function of solar altitude and depth. This permits the simulation of realistic spectral gradients along various temporal and spatial dimensions of the marine environment: diurnal, seasonal, vertical, and latitudinal.
A spectrally sensitive model of photosynthesis is employed to determine the rates at which carbon compounds are synthesized at various points along these gradients. The ratio (ψ) between dinoflagellate and diatom carbon synthesis is determined by taking into account differences in division specific photosynthetic action spectra.

Utilizing this approach, changes in ψ were detected along each of the four dimensions considered in the study. It is assumed that differences in dinoflagellate and diatom carbon synthesis are directly refelcted in the respective population carbon pools. Changes in ψ are taken as an indication of changes in the community composition. The largest changes in ψ were found to occur as a function of depth (22%

maximum difference in daily carbon synthesis), with diatoms being favored with increasing depth. This is interpreted as an indication that the photosynthetic action spectra of the diatoms and dinoflagellates adapt these groups to the lower and upper levels of the water column, respectively. Diurnal changes in ψ were found to be equally large, with diatoms favored in early morning and late evening hours. The relatively slow rates of phytoplankton reproduction preclude the possibility that such changes are significant in establishing diurnal successional patterns. Latitudinal and seasonal changes in ψ were found to be smaller in magnitude than the vertical-diurnal changes. At the equator seasonal changes were negligible. At temperate latitudes changes in ψ indicated a preferential carbon synthesis by dinoflagellates during the winter. This is in conflict with real world observations showing diatom community dominance in the winter. The discrepency is not considered significant as the magnitude of change is small (<2%). At polar latitudes diatoms were favored during the winter and dinoflagellates during the summer. This is consonant with real world patterns of community dominance. Since the magnitude of the changes observed are relatively large at polar latitudes (approaching 10%) the differences in carbon synthesis between the diatoms and dinoflagellates are considered significant. Apparently in polar waters the photosynthetic action spectrum of the diatoms adapts this group to winter light regimes, while that of the dinoflagellates adapts that group to summer light regimes. Thus, phytoplankton seasonal succession can in part be controlled by changes spectral composition and differences in photosynthetic action spectra.

ACKNOWLEDGEMENTS

I would like at the present time to acknowledge the help, support, and assistance which many people have provided during the course of the present study. I would particularly like to thank Dr. Harris White and Dr. Chester Crosch whose detailed discussions and assistance have greatly expedited the successful completion of the work. I would also like to thank the other members of my committee for their consistently helpful advice and discussions. In addition, I would like to thank Dr. C. W. Craven of Science Applications, Inc., for time-off in which to prepare the present manuscript, Mrs. Debbie Danner, Mrs. Marianne Byrnes, Mrs. Reva Underwood, and Mrs. Vicki Hatmaker for their greatly appreciated assistance in the actual preparation of the manuscript.

Finally, and above all others, I wish to acknowledge the debt I owe my wife, Brenda, for her constant support and encouragement, and for putting up with lost nights and weekends for too many years.

TABLE OF CONTENTS

LIST OF TABLES

LIST OF FIGURES

CHAPTER I

INTRODUCTION

The spectral composition of light in the sea varies with several factors. Solar elevation and depth below the surface are of present particular interest because they establish well-defined gradients in spectral composition along several dimensions, including time of day, time of year, latitude, and depth in the water column. This study is primarily concerned with the possibility that such spectral composition gradients are sufficient to produce changes in the composition of the phytoplankton community. This view is predicated upon the assumption that each algal division is characterized by a more or less unique pigment composition (Allan, 1960), and that the interdivisional differences are sufficient to pre-adapt each division for different positions along the light regime spectral gradients. Thus, as the spectral composition varies through time or space, it might be expected that first one, then another, division will be favored. The result would be that the community composition would vary along these gradients. For present purposes this phenomenon is termed "succession."

It is relatively difficult to test this hypothesis in the real world. The fact that responses to factors other than spectral composition vary from division to division, and thus precipitate the same type of composition succession patterns, makes it difficult to provide a well-controlled, real-world test. While laboratory studies can provide

the necessary rigor in experimental control, state-of-the-art problems prevent the realization of spectrally realistic light regimes. Thus, the twin problems of control and realism prevent the resolution of this problem by conventional approaches.

In the present study, these problems are obviated by the application of systems modeling techniques. By restricting the scope of a photosynthetic model to include only variations in light regime, a rigorously controlled experiment can be created. By mathematically modeling the spectral composition of the light regime, a highly realistic photic environment can be provided. While this approach is abstract, it allows the theoretical exploration of an otherwise intractable problem.

Systematic alternation in dominance between algal divisions is a commonplace phenomenon in aquatic communities. In the marine littoral, biomass, and species abundance dominance in the benthic algal community shifts from blue-greens (Cyanophycophyta) to greens (Chlorophycophyta) to browns (Phaeophycophyta) and finally to reds (Rhodophycophyta) with increasing depth (Zaneveld, 1969). The ratio between red and brown algae decreases from low to high latitudes (Chapman, 1957). Similarly, brown algae seem to be favored during the winter months, while red algae seem to be favored in the summer months, at least in the North American temperate latitudes (Hoyt, 1920; Williams, 1948; and Conover, 1958). With respect to the marine phytoplankton community, the ratio between dinoflagellate and diatom cell also shifts. In temperature latitudes the diatoms generally dominate the winter flora, while the dinoflagellates often characterize the summer flora (figure I-1; cf. Riley, 1957; Smayda, 1957; Bogorov, 1958; Margalef, 1958; Rodhe et al., 1958; and

Figure I.1. Seasonal changes in diatom (solid line) and dinoflagellate (dotted line) cell concentrations in Narrangansett Bay. From Smayda 1957.

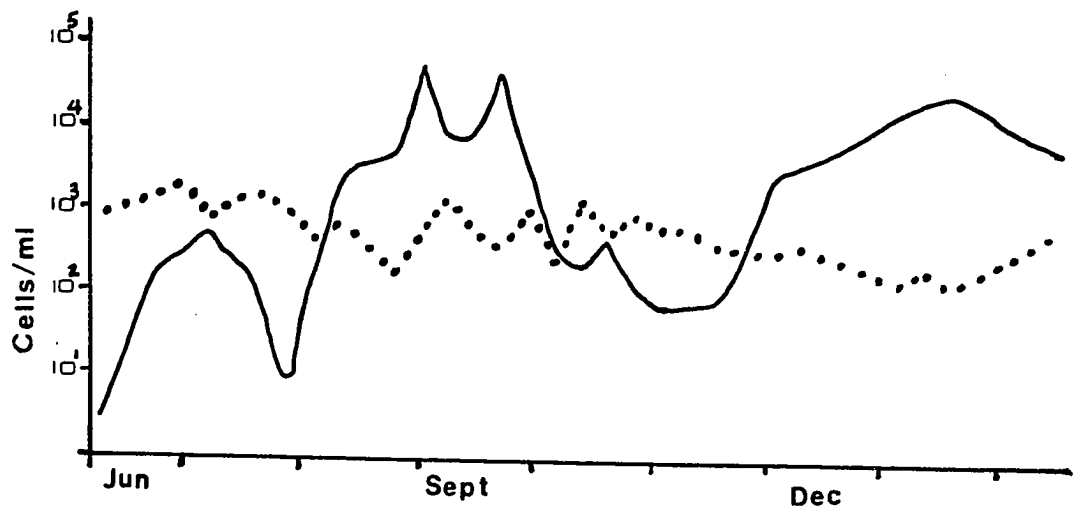

Raymont, 1963). There is also evidence for a decreasing dinoflagellate-diatom ratio with increasing depth (Riley, 1957) and increasing latitude (figure I-2, cf. Hart, 1934).

Since such alternations in composition represent major structural changes in the community it is of interest to identify the regulatory factors. In this regard various hypotheses are present in the literature. The vertical zonation of benthic algae traditionally has been interpreted in terms of spectral composition and intensity of the ambient light regime (Oersted, 1844; Forbes, 1844, Berthold, 1882; Englemann, 1883, von Gaidukov, 1904; and Levring, 1960). Seasonal and latitudinal shifts in benthic algal dominance have been thought of in terms of temperature (Hoyt, 1920; Setchell, 1920). Seasonal changes in the phytoplankton community have been interpreted in terms of temperature (Patrick and Coles, 1969), nutrient status (Pratt, 1965; O'Brien, 1974), zooplankton grazing (Martin, 1970), and light intensity (Riley, 1957; Smayda, 1973; and Hitchcock and Smayda, 1977).

A variety of factors are probably involved in regulating the successional patterns among benthic and planktonic algal divisions. However, it would seem that whatever factors are involved must necessarily possess an intimate relation to algal taxonomy; otherwise their expression would not be observed at such a broad taxonomic level. From this point of view most of the suggested factors seem unlikely candidates. While some show taxonomic affinities (e.g., diatoms as a whole are more cryophillic than dinoflagellates) few possess an intimate taxonomic correlation (e.g., cold preference is not a taxonomic criterion for diatoms).

Figure I.2 Latitudinal changes in the relative composition of the phytoplankton community in the North Atlantic. Plus (+) = diatoms; Dots (.) = dinoflagellates. From Hart, 1937.

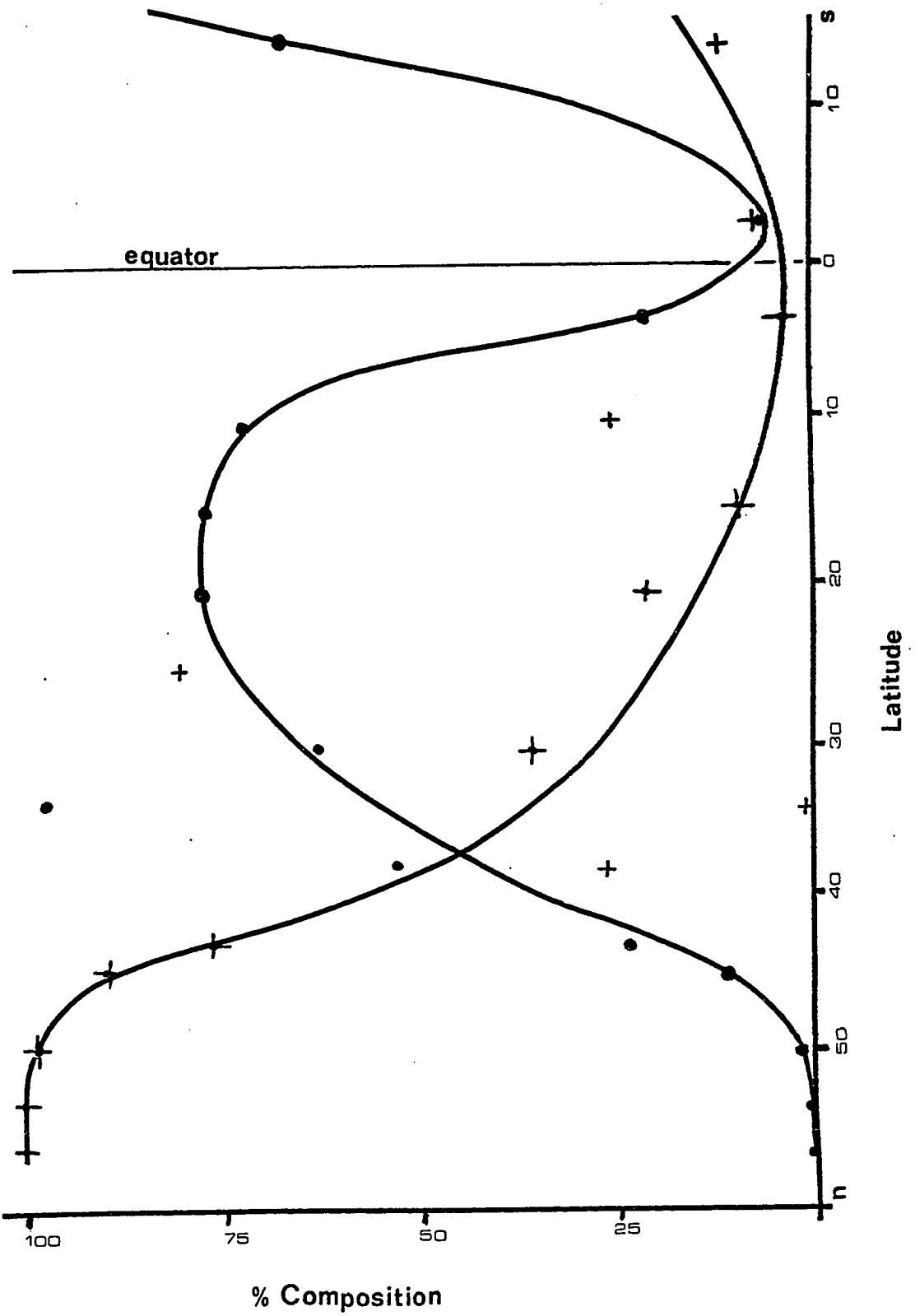

An exception to this is the light regime factor. Pigment composition is critical in establishing the light response capabilities of an alga (Haxo, 1960). It is also a major criterion by which taxonomic distinctions at the division level are made. Thus, there is an intimate link between taxonomic status and light regime response.

The linkage between taxonomic status, composition, and light regime response has been exploited most thoroughly in terms of the vertical zonation of benthic algae. As early at 1844 Oersted suggested that the green-brown-red sequence of benthic algae was a response to differences in the capabilities of these groups to utilize light regimes prevailing at different depths. Near the turn of the century Englemann (1883) and von Gaidukov (1904) proposed that the root of these differences in capability lay in the division specific differences in pigment composition. The work of Haxo and Blinks (1950) rather conclusively established that each of these three algal groups possessed unique patterns of response to light at various wavelengths, and that these patterns of spectral response were consonant with the light regimes prevailing at depths where these groups achieved their greatest relative abundance.

The role of gradients in spectral composition as a forcing function determining the vertical distribution of macroalgae is, then, well-established in the literature. There seems no intrinsic reason why this and similar spectral gradients along other dimensions should not have significance in defining phytoplanktonic community composition. This possibility, has been ignored in the literature. The focal point of the present study, therefore, is an evaluation of the role which division specific differences in photosynthetic action spectrum play in governing phytoplanktonic successional patterns along various spectral gradients.

CHAPTER II

ATMOSPHERIC AND HYDROSPHERIC LIGHT REGIME MODELING

Introduction

In the present chapter formulations are detailed by which the light regime can be modeled for any depth in the water column. There are four discrete steps in this process. First the extraterrestrial light regime at the top of the earth's atmosphere is defined. Second, this light regime is subjected to atmospheric modification generating in the end the light regime at the air-sea interface. Third, the incident light is brought through the interface. Fourth and finally, the sub-interface light regime is subjected to hydrospheric modification, generating an ambient light regime at all depths of interest. Each of these steps will be dealt with in subsequent sections. For convenience a schematic of the processes involved is given in figure II-1.

Extra-Terrestrial Light Regime

The extra terrestrial light regime depends primarily on three factors:

- The solar constant
- The sidereal date
- The spectral composition of sunlight.

The solar constant, F', is the average radiant flux through a unit area normal to the incident light at the top of the atmosphere at mean earth-sun distance, (Coulson, 1975). It's exact value is subject to

Figure II.1. Schematic of the atmospheric and hydrospheric light regime model. Boxes indicate radiation. Ovals indicate control factors.

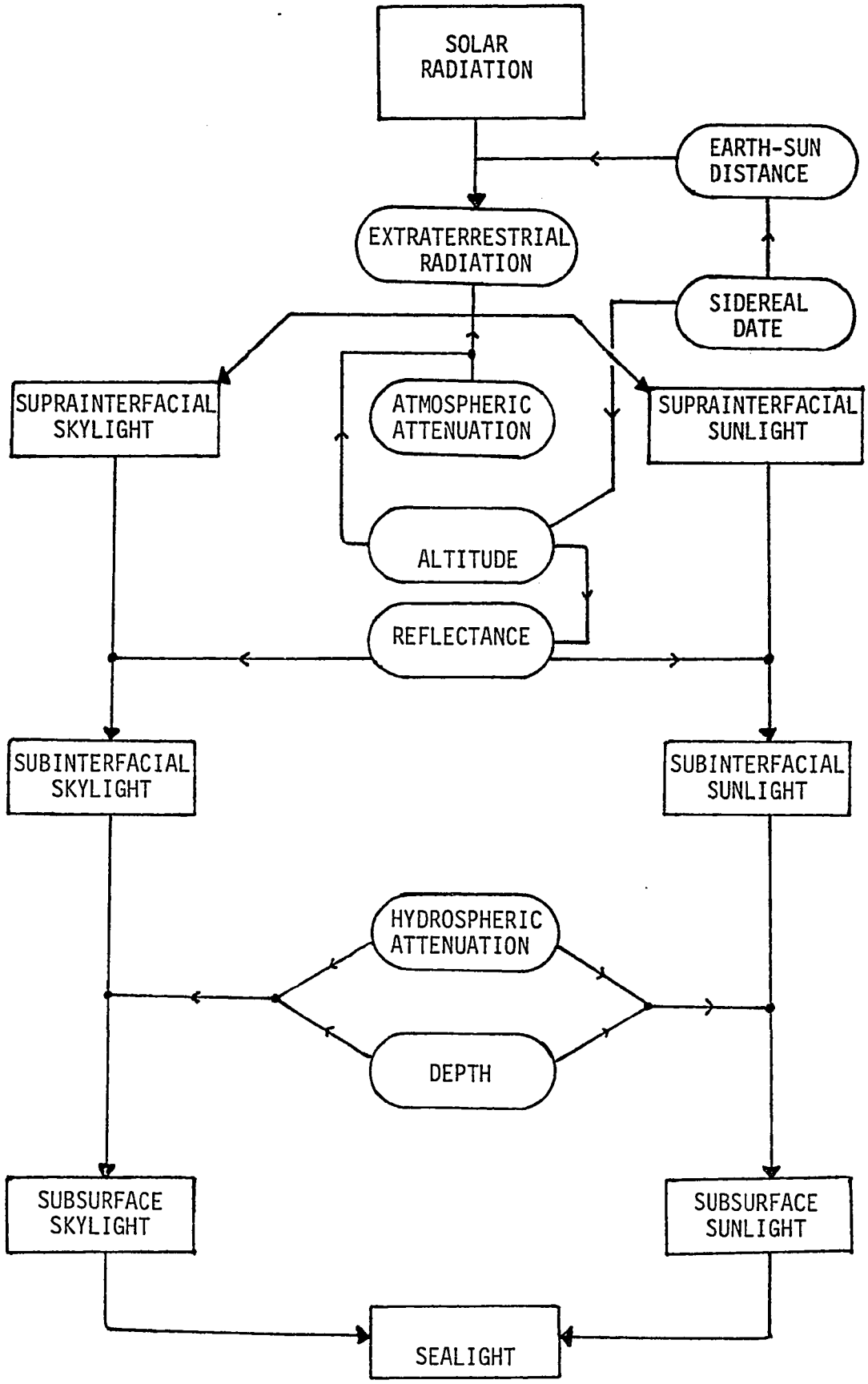

some debate but for present purposes the NASA standard value of 1.940 cal/cm^2/min is assumed (Thekera and Drummond, 1971). Variation in F' due to changes in the earth sun distance amounts to as much as 7% between perihelion and aphelion (Coulson, 1975), and may be adjusted according to

$$F = F'[1.+0.0335 \sin (360\ T/365)] \qquad 2.1$$

The variable T is the sidereal date, or the time in days that has elapsed since the last previous autumnal equinox. September 21.7 is taken as an average value for this event. The error due to this last assumption is generally quite small, introducing a discrepency of no more than two minutes at latitudes less than seventy degrees from the equator (Nassau, 1948).

Given F the extraterrestrial light regime can be generated directly from a knowledge of the spectral composition of extraterrestrial sunlight. Coulson (1975) gives the fraction, ε, by which the various narrow bands of wavelengths (10 nannometer) contribute to the solar constant. The quasi-monochromatic (10 nannometer wave bands) irradiance can be computed as:

$$F_\lambda = \varepsilon_\lambda F \qquad 2.2$$

In nature the range of wavelengths for the extraterrestral light regime extends from about 200 nm (far ultraviolet) to well beyond 1000 nm (far infrared). The photosynthetically active range of wavelengths, however, is much more circumscribed; extending from 300 nm to 730 nm. It is therefore only necessary to employ a light regime model appropriate for

this limited range.

Atmospheric Transmission

Extraterrestrial light passing through the earth's atmosphere interacts with the gas or aerosol particles in three ways:

- Absorption
- Transmission
- Scattering

For the photosynthetically active range of wavelengths absorption is trivial (Coulson, 1975) and can be ignored. The remaining two processes give rise respectively to the direct sunlight and the diffuse skylight components of the atmospheric light regime. Since these two components behave in fundamentally different manners in the atmosphere, in crossing the air-sea interface, and in the hydrosphere, they must be treated separately.

The Direct Sunlight Component

Transmission of light by gas and aerosol particles in the atmosphere produces a direct sunlight component of the atmospheric light regime. For a given wave band centered at wavelength λ, the attenuation of the extraterrestrial monochromatic flux, F_λ, depends on the amount of atmosphere through which the light passes and the wavelength specific mass attenuation coefficient, k_λ. It is convenient to define the atmospheric thickness in terms of the parameter m, the ratio between the slant path distance traversed by the beam through the atmosphere at a solar zenith angle i, and the vertical distance. Several formulations

exist in the literature for defining m as a function of solar zenith angle (see Rosenberg, 1966; Nagel, 1974). Numerical values for a number of these relationships are given in Table II-1. These values may be judged against those of Bemporad which are accepted as the standard of comparison (Rosenberg, 1966; Nagel, 1974). While all the values shown in table II-1 are in good agreement with Bemporad's values, up to i = 70°, only Rozenberg's formulation

$$m = (\cos i + .025e^{-11 \cos i})^{-1} \qquad 2.3$$

affords a good fit at very large angles. It is this relationship, therefore, which will be used in the present model.

The solar zenith angle depends upon latitude ϕ, and the sidereal date, T according to

$$i = 90 - h \qquad 2.4$$

here h is the solar altitude above the horizon as given by

$$h = \arcsin[\sin \phi \sin \delta + \cos \phi \cos \delta \cos (T-\alpha)] \qquad 2.5$$

where, ϕ is latitude, δ is the solar declination, and α is the right ascension, these latter two variables being obtained from an ephemeris for the date in question.

The mass attenuation coefficient, k_λ, is employed to define the optical thickness of the atmosphere, viz.

$$\tau_\lambda = \int_0^\infty k_\lambda \rho \, dz \qquad 2.6$$

Θ	h	N	R	B	L	sec Θ	M
0	90	1.00	1.00	1.00	1.00	1.00	1.00
30	60	1.15	1.15	1.15	1.15	1.15	1.14
45	45	1.41	1.41	1.41	1.41	1.41	1.45
60	30	1.99	2.00	2.00	1.99	2.00	2.18
70	20	2.90	2.92	2.90	2.90	2.92	3.30
75	15	3.81	3.85	3.82	3.81	3.86	4.32
80	10	5.60	5.65	5.60	5.56	5.76	6.03
85	5	10.49	10.40	10.40	10.20	11.5	10.0
86	4	12.60	12.3	12.4	12.1	14.3	11.8
87	3	15.58	15.1	15.4	14.8	19.1	14.4
88	2	19.69	19.4	19.79	18.84	28.6	18.02
89	1	22.93	26.3	26.95	-----	57.3	-----
90	0		40	35-40	44	-----	-----

Table II-1. The atmospheric thickness parameter "m" as a function of zenith angle (Θ = i). Based on various authors: N = Nagel, 1974, R = Rozenberg, 1966, B = Bemporad*, L = Laplace*, M = Muller*. Asterisk indicates data cited by Rozenberg, 1966.

where ρ is the density of air, dz is the depth of the atmosphere traversed, and $k_\lambda \rho$ is the inverse absorption length (i.e., $1/k_\lambda \rho = e$), which is the distance the light travels to be diminished by e. Thus, τ_λ is the attenuation per unit m.

The atmospheric optical thickness, τ_λ, can be fractionated into three components

$$\tau_\lambda = \tau_{R\lambda} + \tau_{A\lambda} + \tau_{0\lambda} \qquad 2.7$$

where $\tau_{R\lambda}$ is due to the Rayleigh atmosphere, (diatomic oxygen, nitrogen, and the noble gases), $\tau_{A\lambda}$ is due to particulate aerosols, and $\tau_{0\lambda}$ is due to triatomic oxygen. A fourth component, $\tau_{W\lambda}$, associated with hydrosols, can be ignored as it is not effective in the photosynthetically active range of wavelengths. The Rayleigh component varies primarily as a function of elevation above sea level. Meterological variation is not significant. Since only sea level elevations are pertinent in the present case $\tau_{R\lambda}$ may be assumed constant. Values for $\tau_{R\lambda}$ used in the model are based on the tabulation provided by Coulson et al. (1960). Similar values for ozone optical thickness, $\tau_{0\lambda}$ are also based on the tabulations of Coulson, et al. (1960). Ozone concentration varies in nature but this is a second order effect (Coulson, 1975) and is ignored. Aerosol optical thickness varies as a function of aerosol load, β, and a particle size coefficient, α'. Angstrom (1961) provides a relationship for determining $\tau_{A\lambda}$ as a function of α' and β.

$$\tau_{A\lambda} = \beta\lambda^{\alpha'} \qquad 2.8$$

The parameter β varies with environmental conditions ranging from 0.000 for an aerosol free atmosphere to 0.200 for an extremely turbid atmosphere. In the present study executions of the model have been performed for these extreme cases and for a value of $\beta = 0.100$. The parameter α' characterizes the modal particle diameter of the aerosol size distribution and varies between zero for small aerosols, and four for large aerosols. Values characteristic of maritime conditions appear not to have been published, but an approximate value can be obtained by fitting Coulson's (1975) values of $\tau_{A\lambda}$ for "Haze M" conditions to equation 2.8 (figure II.2). (Haze M conditions correspond to a maritime environment.) A value of 0.81 is obtained in this manner and is employed in the present model.

Given F_λ, τ_λ, and m, the monochromatic flux in the direct sunlight component, S_λ, can be determined according to

$$S_\lambda = F_\lambda e^{-\tau_\lambda m} \qquad 2.9$$

When S_λ is determined over the range of 300 to 700 nm, the directly transmitted component of the atmospheric light regime in the photosynthetically active range incident on the sea surface is completely defined.

The Diffuse Skylight Component

When a beam of sunlight strikes gas or an aerosol particle, part of the light is scattered out of the direct beam. This scattered light may in turn strike other particles giving rise to second and higher order

Figure II.2. The relation between optical depth and wavelength for a "Haze M" (maritime) atmosphere. Values of optical depth as a function of wavelength are also given for a "Haze C" (continental) atmosphere for purposes of comparison. Based on Coulson, 1975.

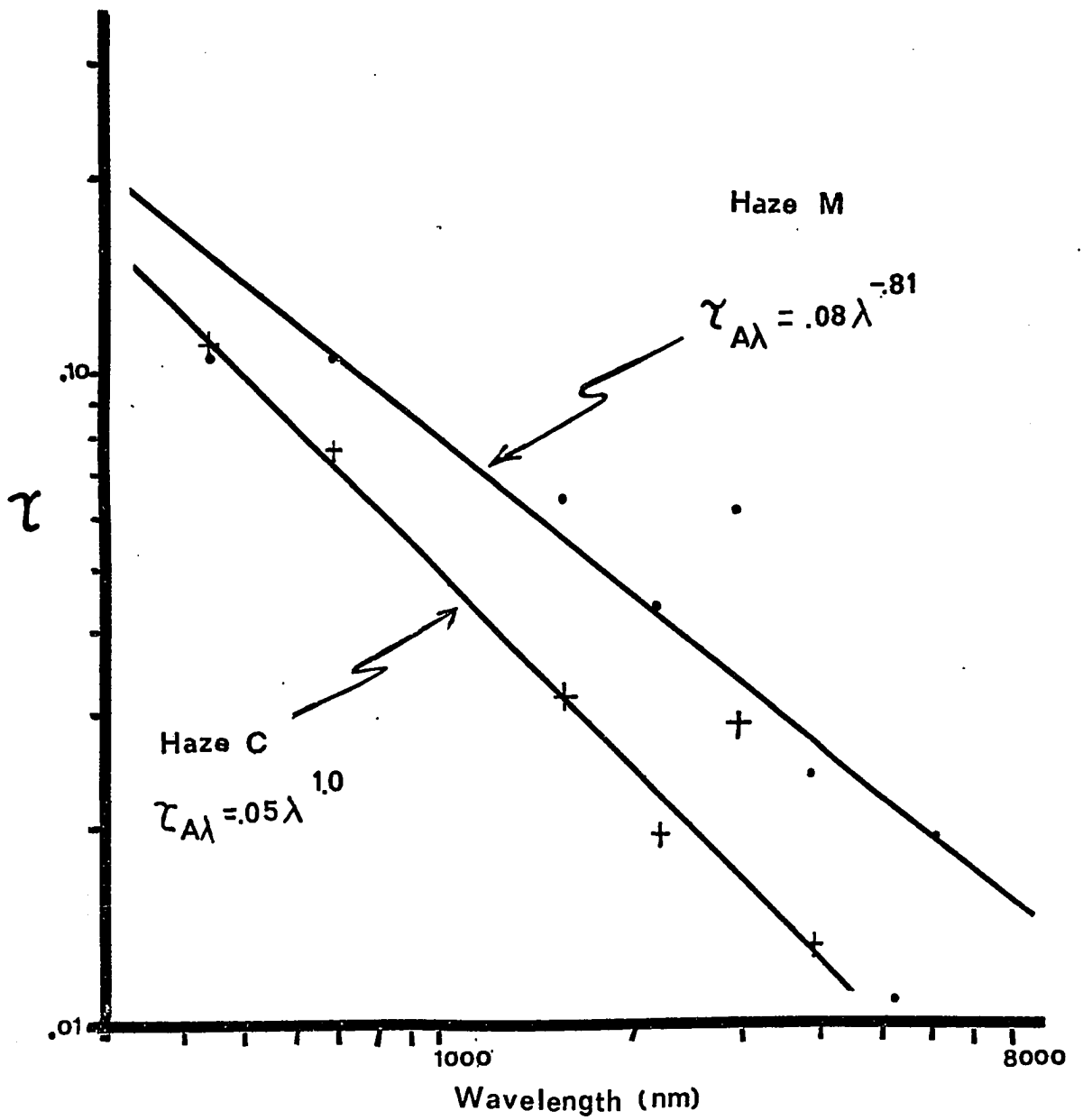

scattering. The net effect is a diffuse skylight component of the atmospheric light regime. The scattered light fields arising from light interaction with gas or aersol particles are somewhat different. It is therefore necessary to describe the diffuse skylight in terms of two separate scattered light fields: the Rayleigh light field associated with Rayleigh scattering centers (oxygen, nitrogen, noble gases, etc.) and the Mie Light field associated with Mie scattering centers (aerosols).

The Rayleigh Light Field. The diffuse skylight, $H_{\lambda R}$, associated with Rayleigh scattering centers can be completely defined (Deirmenjian and Sekera, 1954) according to

$$H_{\lambda R} = \frac{F_\lambda \ (\gamma_1 + \gamma_2)}{m \quad 2(1-\Delta s)} \ -e^{-\tau_{R\lambda} m}$$

where Δ is the sea surface reflectivity, and where

$$s = 1-m_1(K_1+L_1+K_3+L_3) \ -2 \ (K_2+L_2+K_4+L_4) \qquad 2.11$$

$$\gamma_1 = J_1 \ (K_1+L_1) + 2J_2 \ (K_2+L_2) \qquad 2.12$$

$$\gamma_2 = J_1 \ (K_3+L_3) + 2J_2 \ (K_4+K_4) \qquad 2.13$$

$$J_1 = (3/8) \ M_o \ (L_1+L_3) \qquad 2.14$$

$$J_2 = (3/8) \ M_o \ (L_2+L_4) \qquad 2.15$$

The K_ith, L_ith, and M_ith parameters are tabulated by Sekera and Kahle (1966) for various zenith angles and for values of τ. These

values have been incorporated into the model in matrix form. For specific values of τ the appropriate values of K_i, L_i, and M_i are obtained by linear interpolation following McCulough and Porter (1971). Values less than 0.15 are not provided by Sekera and Kahle, but limit values for $\tau = 0.0$ have been computed by means of boundary conditions which they do provide. Interpolations in the region $0 \leqq \tau_{R\lambda} \leqq .25$ are obtained by Lagrangian interpolation. Values of $\tau_{R\lambda}$ are obtained from the tabulation of Coulson et al. 1960.

Over the range of 300 to 700 nm (that is, the photosynthetically active range of light) ozone particles behave essentially as Rayleigh scattering centers in that they are non-absorbing and produce an isotropic (radially symmetric) light field. This permits the application of the Deirmenjian and Sekera formulations in defining the diffuse light field produced by triatomic oxygen scattering centers. In terms of the model this is done simply by summing $\tau_{0\lambda}$ and $\tau_{R\lambda}$ and inserting the result in equation 2.10, for $T_{R\lambda}$. Values of $T_{0\lambda}$ are again obtained from Coulson et al. (1960).

The Mie Light Field. The scattered light field around an aerosol scattering center is strongly anisotropic. The Deirmenjian and Sekera formulations do not hold under these circumstances and it is therefore necessary to provide an alternative method for generating the diffuse light field associated with the aerosols. Twomey et al. (1966) resolve this problem through a matrix method which has been incorporated into the present model.

In the Twomey matrix method the radiation field is approximated by a discrete distribution at points (latitude circles) on the unit sphere,

with matrix relationships defining the incident, reflected and transmitted fields. These matrices are used to satisfy algebraic equations which are then used to compute the properties of thick atmospheric layers built up from thin sublayers, the base of these being a single scattering layer. Directions on the unit sphere are defined in terms of the azimuthal angle, ϕ, and the cosine of the polar angle, μ_i (figure II-3). The multiple-scattering of the radiation field is approximated by scattering of discrete streams in the directions $(\mu_1\phi_1)$, $(\mu_2\phi_2)$... $(\mu_\eta\mu_\eta)$, $(\mu_1\phi_1)$, $(\mu_2\phi_2)$ ...$(\mu_\eta\phi_\eta)$, where negative values are in the downard direction, and positive in the upward direction. Each direction is, in effect, an annular cone, as illustrated in the foregoing figure. Letting the intensity in the direction $\mu_i\phi_i$ be u_i and that in $-\mu_i\phi_i$ be v_i, a transmission matrix $T = [t_{ij}]$ and a reflection, matrix $S = [s_{ij}]$ can be defined for a layer such that an incident radiation field u_o in, for example, the downward hemisphere gives rise to a scattered field Su_o in the upper hemisphere, a diffusely transmitted field Tu_o in the downward hemisphere and a directly transmitted field Eu_o where E is the diagonal matrix with elements $e^{-u}i$. The elements s_{ij} and t_{ij} depend upon τ, albedo, the direction set $(\mu_i\phi_i)$, i=1,2,...N, and the scattering properties of the system. These properties can be described in terms of two matricies, P and B, derived from the phase function p(cosθ) for the maritime haze. A fit to the average phase function for haze M is given by (Grosch, personal communication).

$$p(\cos\theta) = \Sigma C_i \, (1 + g_i^2 - 2g_i \cos\theta)^{-3} \qquad 2.16$$

Figure II.3. The direction scheme for diffuse scattering associated with Mie scattering centers. ϕ is the azimuthal direction while μ is the polar angle.

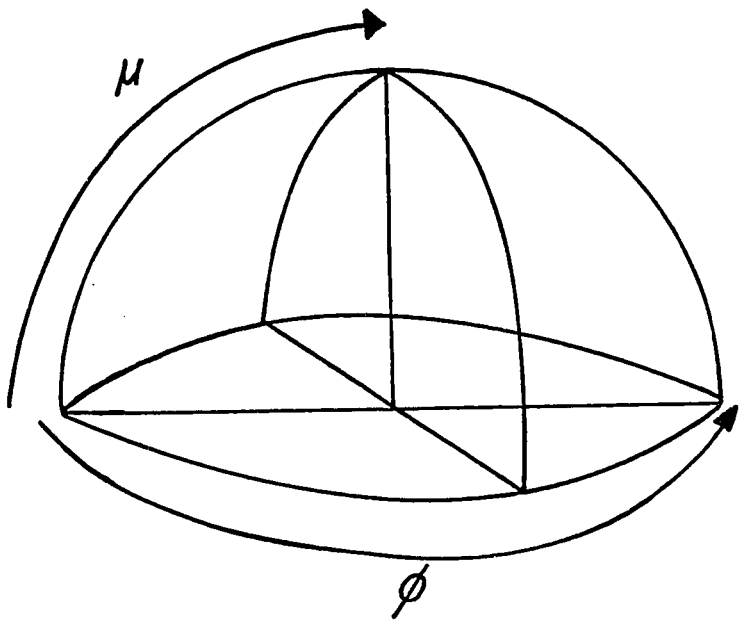

where: i	C_i	g_i
1	$.38267377 \times 10^{-7}$	.91
2	$.19381958 \times 10^{-3}$	.82
3	$.10321609 \times 10^{-1}$	.50
4	$.33784933 \times 10^{-3}$	.50

The parameter θ_{ij} is the arc-cosine of the product $\hat{p}_{ij} = \mu_i\mu_j$ or $\hat{b}_{ij} = -\mu_i\mu_j$, where $\hat{p}_{ij}$ is the fraction of energy removed from the j^{th} direction and reappearing in the i^{th} direction with the same sense, and $\hat{b}_{ij}$ is the fraction reappearing in the i^{th} direction but in the opposite sense to the original radiation. The matrices P and B are obtained by taking all permutations of u_i and u_j such that:

$$\mu_i = .05 + i(.1) \qquad i = 0,1...8$$
$$\mu_j = .05 + j(.1) \qquad j = 0,1...8$$

The transmission and scattering matrices, S and T, are obtained directly from P and B for a thin scattering layer of thickness $\Delta\tau$ according to

$$S = M^{-1}B\,\Delta\tau \qquad 2.17a$$
$$T = M^{-1}P\,\Delta\tau \qquad 2.17b$$

where M is the diagonal matrix with elements μ_i.

Consider a layer of thickness t_1 with characteristic scattering matricies S_1 and T_1. An intensity vector v falling upon this layer gives rise to radiation S_1v representing backscatter, E_1v representing direct transmission through the layer, and T_1v representing forescattering through the layer. If a second layer of thickness t_2 and characterized by matricies S_2 and T_2 is present below the first, T_1v and E_1v will be partially transmitted, partially reflected and partially scattered giving rise to additional radiant fields directed upon the first from below. As this progressive divisional process continues a complex radiant field is created. Since the two layer combination is equivalent to a single layer of thickness t_1+t_2, and v is arbitrary, the overall relationship between S, T, and E can be written.

$$S = S_1 + (T_1+E_1)S_2(I+S_1S_2+(S_1S_2)^2+\ldots)\,(T_1+E_1) \qquad 2.18a$$

$$T = (T_2+E_2)(I+S_1S_2+(S_1S_2)^2+\ldots)(T_1+E_1) - E \qquad 2.18b$$

If T_2 is made infinitesmal, and noting that for an infinitesimal layer the matrix E becomes $I-M^{-1}\,\Delta\tau$, the relationships in 2.17a can be used in 2.18 for S_2 and T_2 obtaining

$$S + \frac{\partial S}{\partial \tau} = S + (T + E)M^{-1}_{B}(I+\ldots)\,(T+E) \qquad 2.19a$$

$$M\frac{\partial S}{\partial \tau} = M\,(T+E)\,M^{-1}\,B(T+E) \qquad 2.19b$$

$$M\frac{\partial T}{\partial \tau} = -T + (P + MSM^{-1}B)\,(T+E) \qquad 2.19c$$

To determine the diffuse skylight associated with the Mie atmosphere a set of transmission matrices for various values of $\tau_{A\lambda}$ (.1, .5, 1.0, 2.0...) are obtained by integrating 2.19 b,c from zero to the value of $\tau_{A\lambda}$ of interest. Transmission matrices for intermediate values of $\tau_{A\lambda}$ are obtained by interpolation. In this way a matrix T can be obtained for any given value of $\tau_{A\lambda} = \tau_i$. The diffuse skylight associated with τ_i can thus be obtained by multiplying T' by the diagonal matrix U of elements u_i and summing over all values of j:

$$H_{\lambda A} = \Sigma U \, T_j \qquad 2.20$$

The Diffuse Light Field. Once the Rayleigh and Mie light fields have been determined the overall diffuse light field is obtained by simple summation,

$$H_\lambda = H_{\lambda R} + H_{\lambda A} \qquad 2.21$$

It should be noted that this approach assumes that the Rayleigh and Mie atmospheric components interact independently with the light field. In fact, there is a degree of dependent interaction; e.g., a photon scattered by a Rayleigh scattering center may latter be scattered by either a Rayleigh or a Mie scattering center. It is assumed that this interdependance is effectively minimal.

Hydrospheric Transmission

The foregoing relationships determine the monochromatic flux at the sea surface at a given point in time and space. Since the physical

properties governing the behavior of the direct and diffuse components are different within the hydrosphere as well as the atmosphere, their separate identities must be maintained.

The Direct Sunlight Component

If it is assumed that the air-sea interface is flat, its reflectance for direct sunlight, R_s, is given by Jerlov (1968):

$$R_s = (\sin(i-j)^2/\sin(i+j)^2+\tan(i-j)^2/\tan(i+j)^2)/2 \qquad 2.22$$

The wavelength dependence of reflectance is assumed negligible (Jerlov, 1968). The parameters i and j represent the angles of incidence and refraction (figure II.4). The parameter i is, of course, the zenith angle as previously determined (equations 2.4 and 2.5). The parameter j is given by Snell's law:

$$j = \arcsin(\sin(i/r) \qquad 2.23$$

where r is the refractive index of the medium, here assumed invariant as 4/3 (Jerlov, 1968). Given R_s, and the incident monochromatic irradiance, $S_{\lambda p}$, the penetrant beam irradiance, $S_{\lambda \rho}$, is given by:

$$S_{\lambda p} = S_{\lambda \rho} = R_s \, S_{\lambda i} \qquad 2.24$$

Figure II.4. Sea surface refraction. The angle of incidence = zenith angle = i; the solar altitude = k; the angle of refraction = j; the vertical depth = z; and the attenuation distance is z'.

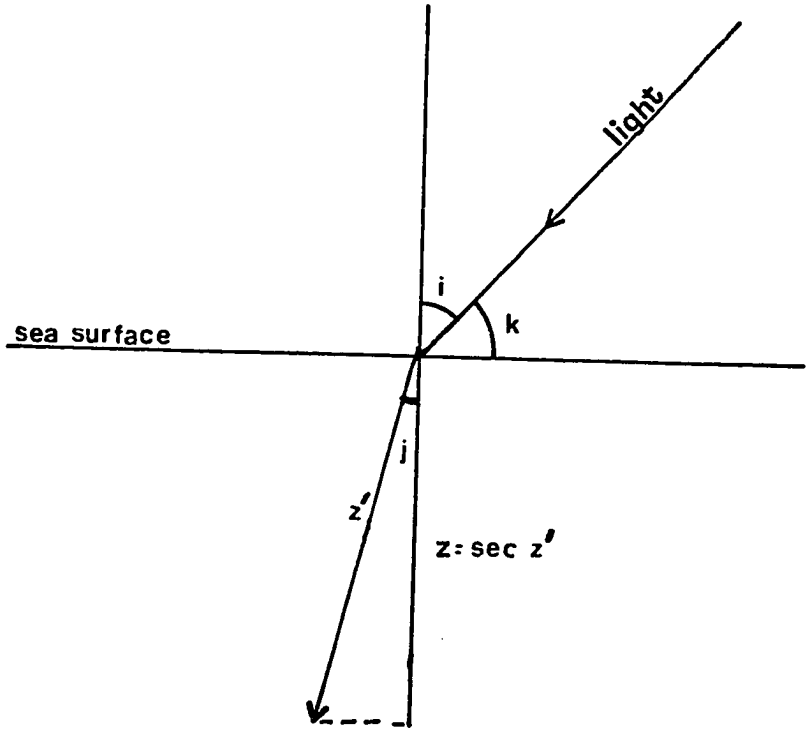

The contribution of the penetrant sunlight to the irradiance at depth z depends upon the attenuation coefficient α_λ and the angle of refraction. Attenuation coefficients, such as provided by Jerlov (1968) and here employed, account only for the diminution of the beam irradiance; they ignore the possibility of secondary backscatter onto the target of scattered beam irradiance due to suspended particles. Shannon (1975) provides a correction for this phenomenon with the relationship:

$$K_\lambda = .02\ \alpha_\lambda + .04 \qquad 2.25$$

The total irradiance on the target area derived from the direct beam irradiance is then determined from:

$$S_{\lambda z} = S_{\lambda p}\ e^{-K_\lambda\ z\ \sec\ (j)} \qquad 2.26$$

The Diffuse Skylight Component

Since the diffuse portion of the global irradiance incident upon the sea surface comes from all portions of the global hemisphere, reflectance is somewhat more difficult to handle than with the direct sunlight component. However, Burt (1954) has examined this problem and has found that for flat sea surfaces, and clear skies, as here assumed, the reflectance of the diffuse skylight, R_h, assumes a more or less constant value of 6.6% of the total diffuse skylight, H_λ, as:

$$H_{\lambda p} = H_{\lambda i} - 0.066 H_{\lambda i} \qquad 2.27$$

As a practical matter it is convenient to assume that the penetrant diffuse skylight is uniformly directed downward along the vertical. In this case the diffuse skylight remaining at depth z is defined according to the exponential decay function:

$$H_{\lambda Z} = H_{\lambda p}\, e^{(-K_{\lambda}\, z)} \qquad 2.28$$

Ambient Light Regime At Depth

In so far as I am aware there is no study in the literature purporting to show that phytoplankton are capable of discriminating between direct and diffuse radiation. It therefore seems reasonable to sum the diffuse and direct irradiances once they have been computed for a specific target depth. The parameter G_{λ}:

$$G_{\lambda} = H_{\lambda} + S_{\lambda} \qquad 2.29$$

is taken as the primary in-put and forcing function for the photosynthetic submodel described in the following chapter.

CHAPTER III

PHOTOSYNTHETIC MODELING

Introduction

There is a large body of literature dealing with the photosynthetic responses of phytoplankton as a function of total light energy. This literature has been reviewed recently by Patten (1968) and Dugdale (1975). Those models currently in use in the literature for simulating the photosynthetic responses of the phytoplankton ignore, without exception, wavelength dependencies inherent in the photosynthetic process. Such models are capable of discriminating between response of various algae only in terms of light intensity parameters. They are not capable of such discrimination in terms of photosynthetic action spectrum differences. In the present chapter the extant photosynthetic light intensity models will be reviewed, and an appropriate adaptation to account for wavelength dependencies provided.

Existing Photosynthetic Models

The Light Response Curve

There are two basic approaches in use for defining the photosynthetic response of organisms in terms of light intensity. The first of these, mentioned here only in passing, is the kinetic approach wherein the molecular processes underlying the response are rigorously defined. This approach has been developed in particular on the basis of the work of Baly and Morgan (1934), Emerson and Green (1934), Baly (1935), and

Burk and Lineweaver (1935), and is useful in elucidating the biochemical processes involved. Researchers working in ecological contexts have exclusively employed an empirical, or "black box", approach, in which observed responses under varying light intensities are simulated through numerical analogs. Figure III.1 provides a schematic diagram of a typical photosynthetic-light intensity response curve. Three distinct regions of this curve are recognized:

1. The suboptimal region---photosynthetic response increases with increasing intensity,
2. The optimal region---maximum photosynthetic response is obtained and the system is light saturated,
3. The supraoptimal region---increased light intensity in this region produces a photoinhibitory effect acting to depress the PS-LI curve.

The parameters I and P represent, respectively, the light intensity ($cal.cm^{-2}$ $min.^{-1}$), and photosynthetic rates (mg carbon/unit time). The parameters I_m and P_m represent the light saturation intensity and the light saturated photosynthetic rate; that is, the maximum photosynthetic rate which the system can achieve (P_m) obtains at the light intensity I_m. A useful parameter is I_k, which defines the shape of the curve in the suboptimal region. It is defined as the intersection of the "initially linear portion of the curve" with the p_m isocline. There are no generally accepted parameters defining the photoinhibitory region, but for present purposes I_i and I_t, representing the intensities at which incipient and total inhibition are achieved, are of use.

Figure III.1. Changes in carbon synthesis rate (P) as a function of light intensity. P_m = maximum synthesis rate. I_k = intensity at which tangent to curve at origin intersects P_m isocline. I_m = intensity at which maximum carbon synthesis rate (P_m) is achieved. I_i = intensity at which photoinhibition is initiated. I_t = intensity at which total photoinhibition occurs.

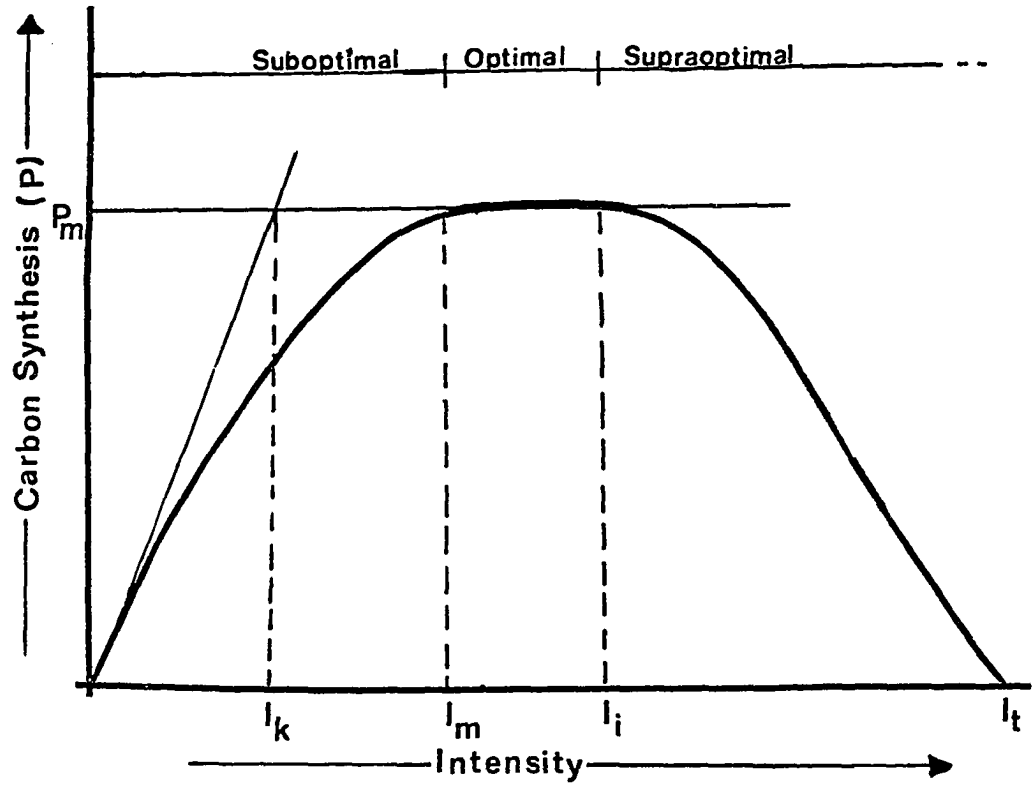

Light Saturation Models

Idso and Foster (1975) have described the existing light intensity response models as belong to one or another of three classes (illustrated in figure III.2). The first of these classes utilizes "light saturation" formulations which define only the suboptimal and optimal regions of the curve (curve I of figure III.2). E.I. Smith (1936, 1937, 1939), working on the numerical foundation laid down by Hecht (1923, 1935) for photosensory response analogs, pioneered in this area, writing:

$$P = KIP_m/(1+K^2I^2)^{\frac{1}{2}} \qquad 3.1$$

where K is a proportionality fraction defining the shape of the curve, representing some arbitrarily selected proportion of Pm Talling (1957a,b) reduced the arbitrary quality of the K parameter by setting $K=I_k$, where I_k is as previously defined. With Talling's modification, the Smith model becomes:

$$P = I\ P_m/I_k(1 + I^2/I_k^2)^{\frac{1}{2}} \qquad 3.2$$

The curve generated by the Smith-Talling model is hyperbolic, a fact which is in accordance with biological reality in the sub-photoinhibitory region. Recently Jassby and Platt (1956) have taken cognizance of this point and have provided an alternative simplified expression:

Figure III.2. Various classes of photosynthetic response models. Class I, Light Saturation, assumes no photoinhibitory effects. Class II, Asymptotic Inhibition, assumes that under photoinhibitory light intensities photosynthetic response approaches zero asymptotically. Class III, Total Inhibition, assumes that photosynthetic response under photoinhibitory light intensities drops to zero at some finite intensity.

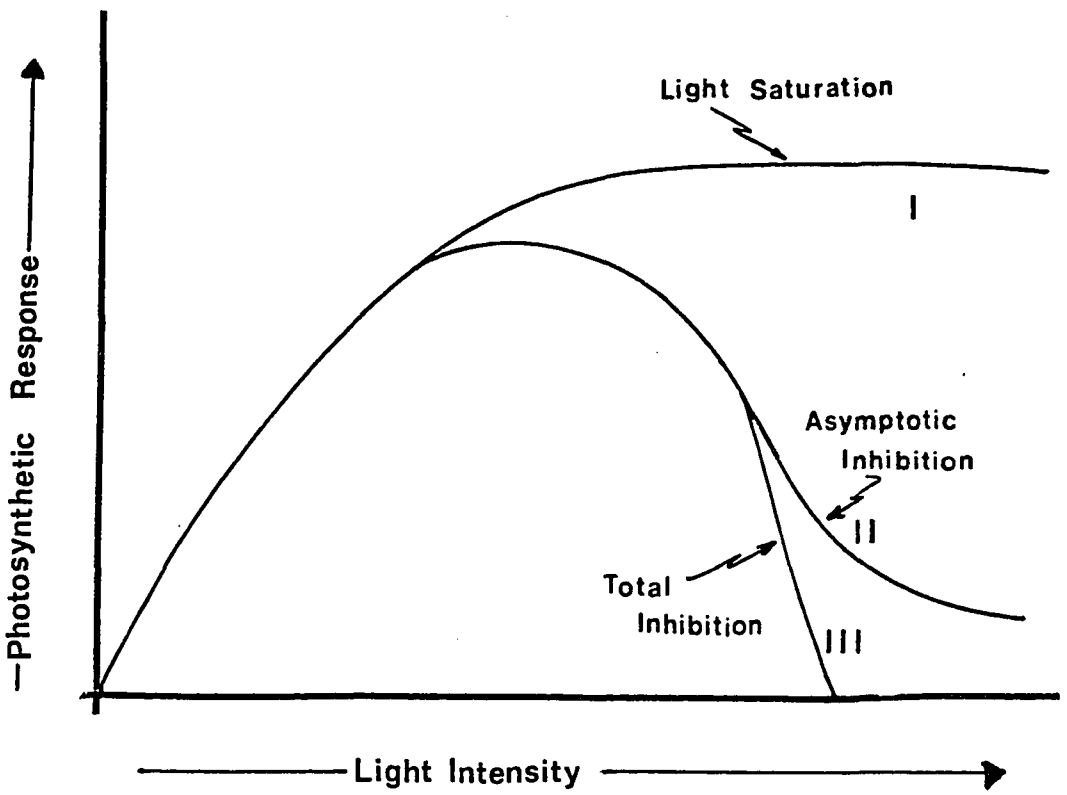

$$P=P_m \tanh (I/I_k P_m) \qquad 3.3$$

The Smith-Talling and Jassby-Platt models predict that P approaches p_m asymptotically with increasing light intensity. While this ignores photoinhibition effects, the curves generated by these models are quite similar to those observed in the laboratory (cf. Myers and Burr 1941, Qasim et al. 1972, and Dunstan 1976). Jassby and Platt have evaluated each of these curves with data from the natural environment and have found that their own model produces a somewhat better simulation than that of the Smith-Talling model.

Asymptotic Inhibition Models

Idso and Foster's second class of models are those in which the entire curve is simulated, but it is assumed that in the supraoptimal region P decays asymptotically with light intensity (curve II of figure III.2). Steele (1962) appears to have been the first worker to attempt to incorporate a photoinhibitory effect at high light intensities. The model which he employs abandons the hyperbolic curve in favor of an exponential curve generated according to the relation:

$$P=(I/I_m)\, e^{(-I/I_m)P_m} \qquad 3.4$$

Jassby and Platt extended their analysis of light curve models to include that of Steele, considering only the suboptimal and saturation region for the curve generated by equation 3.4. Their findings show that the Steele model does not provide a good simulation in this region.

Vollenweider (1965) provides the following relationship:

$$P = P_o I\ (1 + I^2/I_k^2)^{-\frac{1}{2}}(1 + a^2I^2)^{-n/2} \qquad 3.5$$

The Vollenweider model has the advantage of retaining the widely accepted hyperbolic form of the light response curve. Indeed, it is equivalent to the Smith-Talling model when n=o, since P_o is related to P_m according to Fee's (1969, 1973) relationship:

$$P_o=(P_m/I_m)\ (1+I_m^2)\ (1 + a^2 I_m^2)^n \qquad 3.6.$$

The Vollenweider model has had widespread acceptance in the literature, and has been applied in phytoplankton production model contexts in a number of instances, (e.g., Vollenweider, 1965; Fee, 1963, 1973; Lewis, 1974; Bannister, 1974a, b; and Winter et al. 1975). Unfortunately, the parameters a and n presently lack biological meaning (Ganf, 1975), thereby reducing the general applicability of the model.

Idso and Foster (1975) provide yet another approach to simulating the light response curve, writing:

$$P=P_m \sin (3.12\pi\ I) \qquad I<0.16 \qquad 3.7a$$

$$P=P_m\ (.64 + 0.36 \sin (3.12\pi\ I) \qquad 0.16<I<0.32 \qquad 3.7b$$

$$P=P_m\ (0.64\ e^{-6.24\ (I-.032)}) \qquad I>0.32 \qquad 3.7c$$

Where the numerical limits are empirically determined values in units of $cal.cm^{-2}\ min^{-1}$. This use of specific values severely reduces the generality of the model making it inconvenient to apply it in other contexts, though the authors have found it of great use in their own work.

Total Inhibition Models

At the present time, our understanding of the photoinhibitory portions of the PS-LI response curve seems incomplete. Asymptotic models described in the literature perhaps have been adopted as a matter of convenience, or possibly in conformance with the well known curves published by Riley (1957). Given the relative paucity of data points at extreme intensities scrutiny of Riley's original data (Figure III.3) suggests that an asymptotic curve is not particularly appropriate. From an intuitive point of view it is difficult to conceive how carbon synthesis could persist at extreme intensities, which is the case implied by the asymptotic models. Further, the data from Kok (1956) (figure III.4) demonstrates the existence of an intensity at which oxygen evolution (hence carbon synthesis) does drop to zero.

The foregoing suggests that a total inhibition model would be the most appropriate choice for incorporation into a photosynthetic model (curve III of figure III.2). In so far as I am aware the only model of this type extant in the literature is that proposed by Idso and Foster (1975):

$$P = P_m \sin (3.12\pi I) \qquad 3.8$$

Figure III.3. Photosynthetic response as a function of light intensity based on Ryther's (1956) data. Curve A corresponds to Ryther's asymptotic interpretation. Curve B corresponds to a total inhibition interpretation.

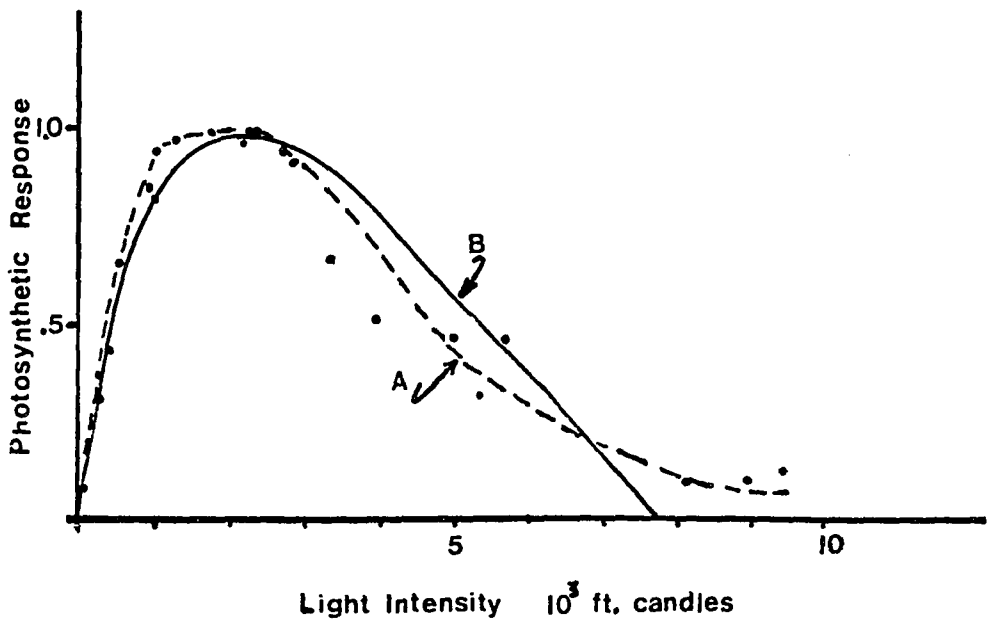

Figure III.4. Photosynthetic oxygen evoution as a function of light intensity (solid line). Dashed line represents zero oxygen production or consumption. Values of oxygen evolution on plus (+) side of dashed line indicate oxygen production. Values on minus (-) side of dashed line indicate oxygen consumption. Based on Kok (1956).

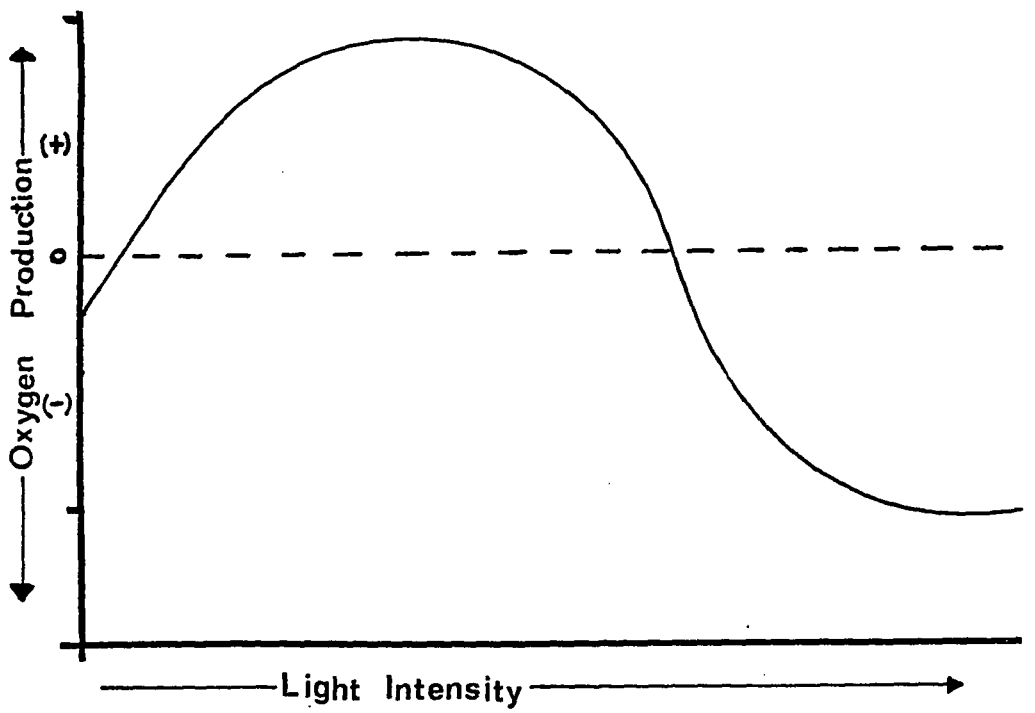

Since the Idso-Foster total inhibition model generates an endless sine wave (figure III.5) it is necessary to specify boundary conditions with other models being employed to describe the sub-photoinhibitory region of the PS-LI response curve.

A Wavelength Sensitive Model

In the present section a model suitable for generating monochromatic photosynthetic light response curves will be presented. Relatively little work has been done in this area as the necessary empirical studies upon which to base such models are uncommon. Certain theoretical characteristics of these curves are, however, generally accepted. In particular, at saturating light intensities it is thought that the response becomes independent of wavelength, and is a function only of total intensity. This point is clearly shown in the work of Pickett and Myers (1966), who provide monochromatic curves for several wavelengths, (figure III.6). McCleod (1961) has reported that at light saturated intensities, a certain degree of action spectrum structure is retained, and the curves are not totally flat, but the degree of departure from theoretical expectations is small, and will be ignored. Inspection of Pickett and Myer's curves suggests that they can be adequately modeled by means of light saturation type formulations as long as the total light intensity is less than I_i. Since the Jassby-Platt model provides a closer approximation of real world responses in this region of the polychromatic curve, it will be used as the basis for present work. The necessary parameters for the Jassby-Platt analog are I, I_k and P_m. Analogous terms in a monochromatic context would be I_λ, $I_{k\lambda}$ and $P_{m\lambda}$. I_λ is, of course, obtained from the atmospheric and hydrospheric

Figure III.5. Photosynthetic response as a function of light intensity, assuming Idso and Foster's (1975) total inhibition model.

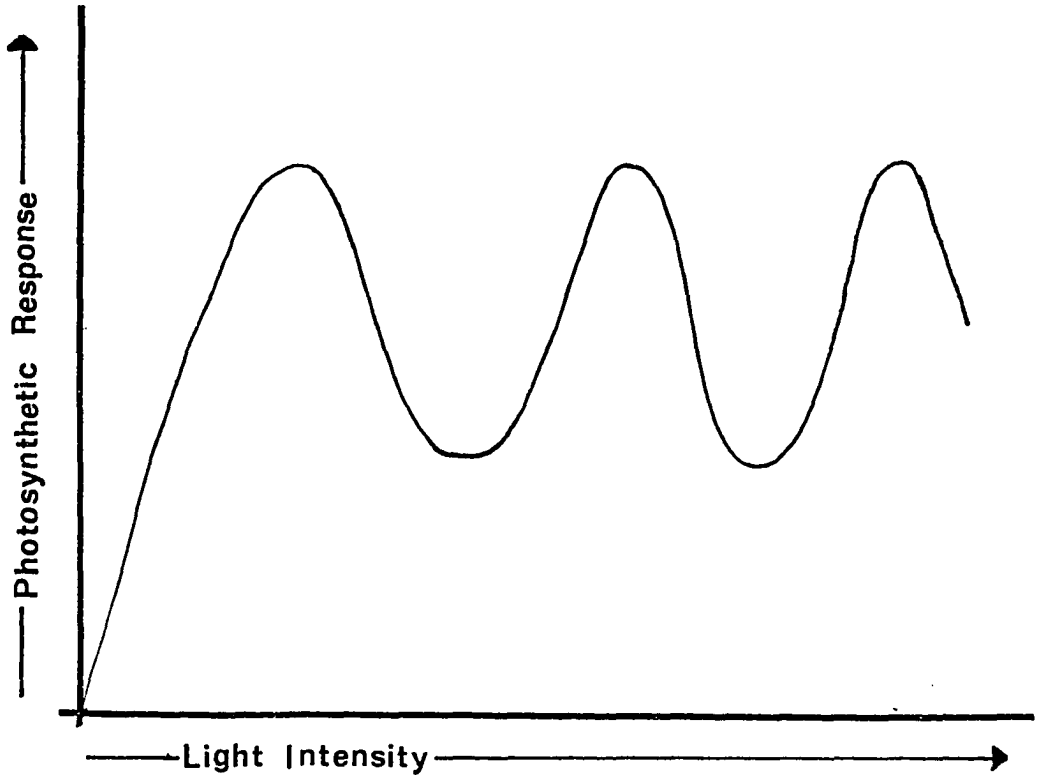

Figure III.6. Photosynthetic response as a function of light intensity using quasi-monochromatic light. Curve a = 450 nm; curve b = 525 nm; curve c = 575 nm; curve d = 630 nm; curve e = 650 nm; curve f = 680; curve g = white light.

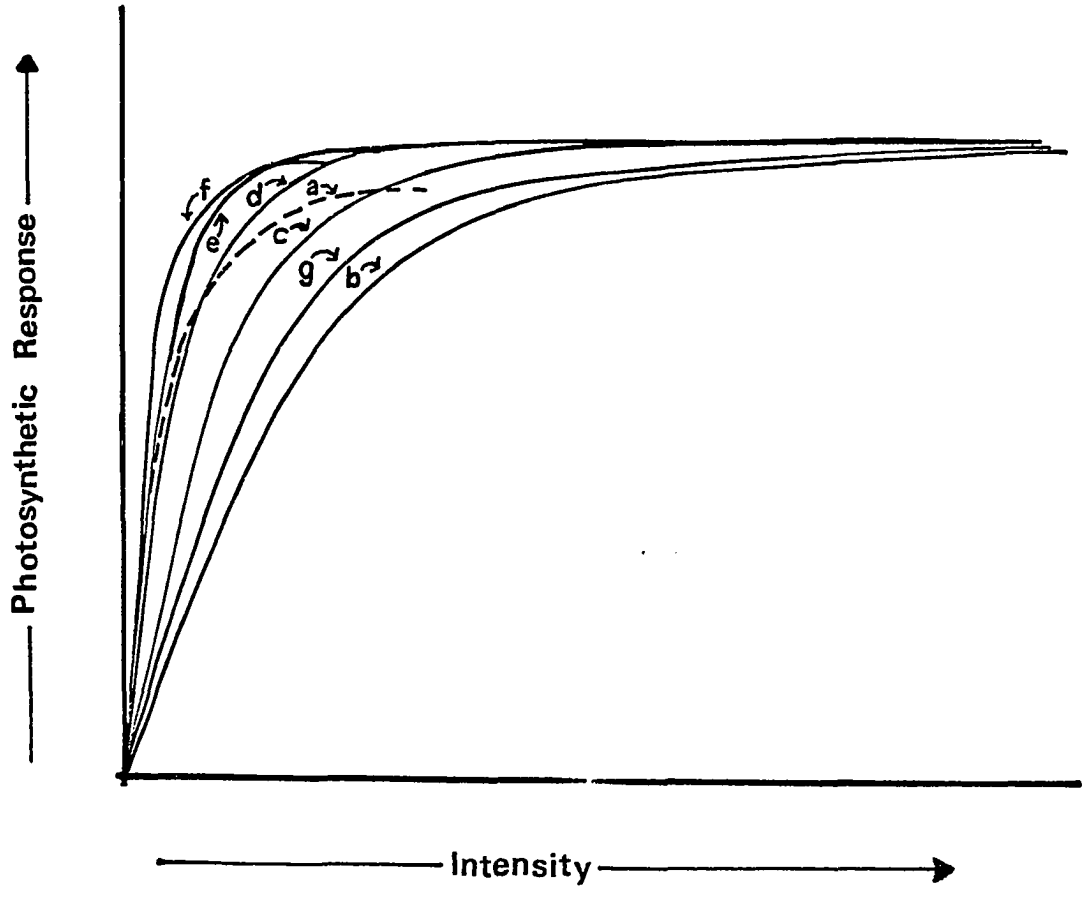

submodels of ambient light regime. $I_{k\lambda}$ and $P_{m\lambda}$ are related to empirically determined values of I_k and P_m. Since $P_{m\lambda}$ is essentially independent of wavelength it is convenient to set it equal to unity. Under these circumstances it is clear that $I_{R\lambda}$ must be a function of the photo-synthetic action spectrum, otherwise the curves in III.5 could not be produced. It is now convenient to define a function f_λ such that

$$f_\lambda = P_\lambda / P_r \qquad 3.9$$

where P_r, and P_λ represents the photosynthetic responses of a specific organism at some low intensity for the wavelength of interest, r, and a reference wavelength, r. P_r can be selected from a limited number of values for specific wavelengths given by Pickett and Myers. Measurements of P_λ at low light intensities are available in the literature for a variety of divisions (see Haxo 1960). A purely empirical relation can be shown appropriate for relating F_λ and $I_{k\lambda}$:

$$I_{k\lambda} = I_{kr} / f_\lambda^{(2/3)} \qquad 3.10$$

Figure III.7 compares the values obtained by this relationship with those provided by Pickett and Myers' data. The fit seems quite reasonable. That such a relationship can be written allows the Jassby-Platt model to be rewritten so as to take advantage of this fact:

$$P = P_{m\lambda} \tanh(I / I_{k\lambda} P_{m\lambda}) \qquad 3.11a$$

Figure III.7. The relation between photosynthetic action spectrum and $I_{k\lambda}$. Solid line represents data from Pickett and Myers (1966). Dashed line represents theoretical values according to equation 3.10.

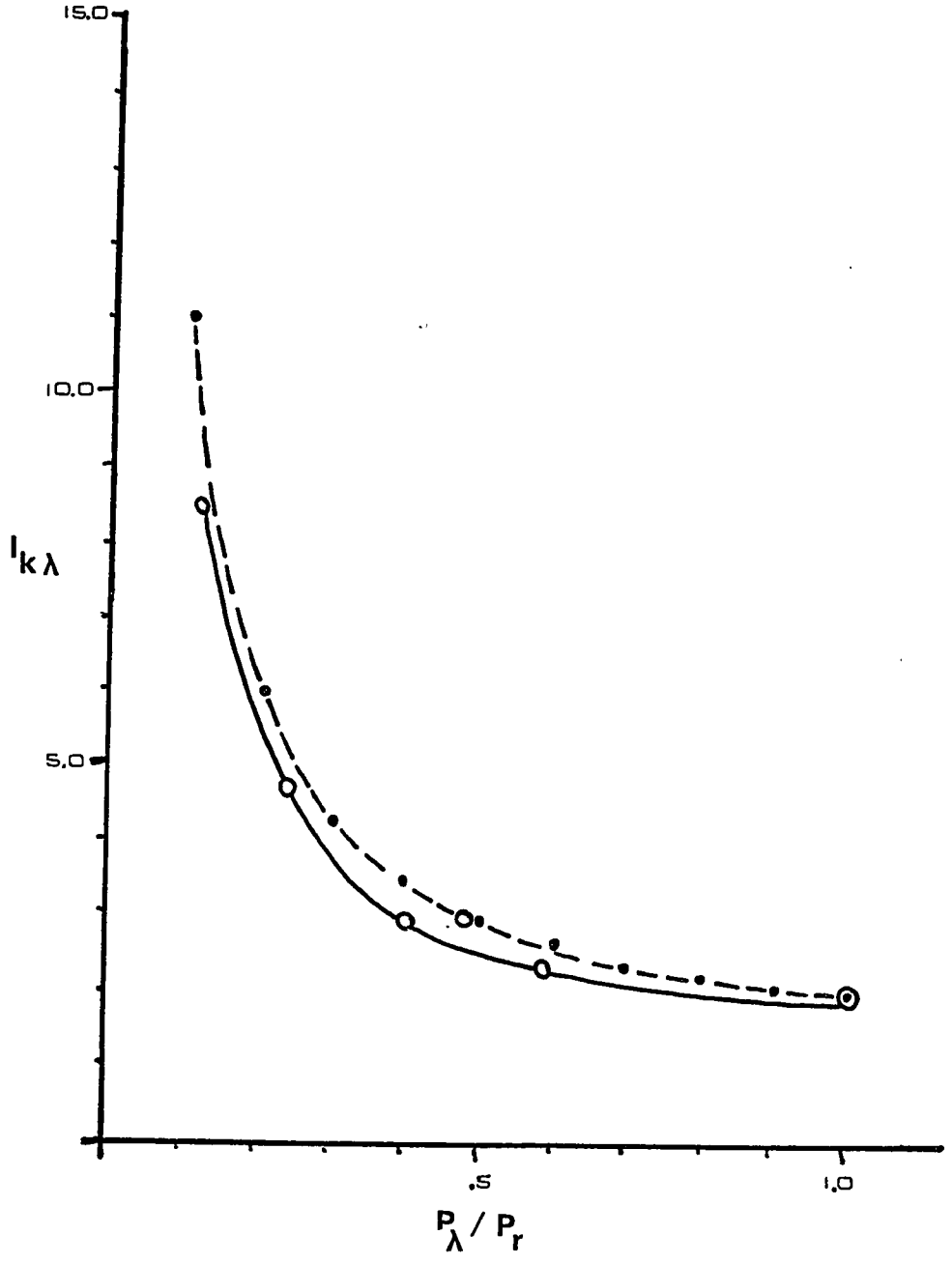

or, with $P_{m\lambda} = 1.0$

$$P = \tanh (I/I_{k\lambda}) \qquad 3.11b$$

Equation 3.11 a,b can be employed to generate the monochromatic photosynthetic response curve for any wavelength in the photosynthetically active range up to $I=I_i$. Because P approaches P_m asymptotically a slight discontinuity in the response curve exists at I_h, though this should have no practical consequence for simulating real world responses.

A different model is required if photoinhibition is to be simulated. It is convenient, if esthetically unappealing, to utilize 3.11 a,b in the sub- and optimal regions, and a second analog in the photoinhibitory region. At the present time, there seems to be no truly definitive study of photoinhibition in algae, so that the selection of an appropriate model in this region is somewhat arbitrary. Asmyptotic inhibition seems unreasonable on theoretical grounds previously discussed. Idso and Foster's concept of total inhibition seems much more acceptable, but the model which they employ is somewhat unsatisfactory, as it predicts alternating positive and negative response over the entire photoinhibitory region. Therefore, in the absence of a suitable model in the extant literature it will be assumed that photoinhibition follows the relationship:

$$F'' = [1-(I-I_t)]^2 \qquad 3.13$$

where F" is an inhibition function active between I_i and I_t such that:

$$P = P_m F" \qquad 3.14$$

Below I_i equation 3.12b applies, and above I_t

$$P = 0.0 \qquad 3.14b$$

Thus the monochromatic light intensity response curve is completely defined by equations 3.12b, 3.14a, and 3.14b.

System Parameters

Photosynthetic Wavelengths

Photosynthetic models in the extant literature employ total light irradiances in the range of 400 to 700 nannometers. This is usually considered to be the photosynthetically active range of wavelengths, but work by McCleod (1958), McCleod and Kanwisher (1962), and Halldal (1968) shows that carbon assimilation is significant in diatoms and dinoflagellates down to 300 nannometers. There are also indications in the literature that photosynthesis extends upward into the near infra-red as far as 730 nm, (Haxo, 1960; Mann and Myers, 1968; Halldal, 1968; and Iverson and Curl, 1973). It is therefore necessary to include the entire range of wavelengths from 300 to 730 nannometers in the PAR.

Photosynthetic Action Spectrum

A critical aspect of the photosynthetic model is the action spectrum selected. Differences in photosynthetic efficiency at different wavelengths have long been noted. Haxo and Blinks (1950) demonstrated that division specific action spectrum differences existed among the algae by providing extensive measurements of photosynthesis at short wavelength intervals. There are now numerous studies in the literature providing action spectra for the Chlorophycophyta, Phaeophycophyta, and Rhodophycophyta, (Haxo and Blinks, 1950; Yoccum and Blinks, 1954; Haxo, 1960; Fork and Amesz, 1967; and Halldal, 1969). Despite the great importance of diatoms and dinoflagellates in the marine ecosystem there has been relatively little work with these groups as far as action spectra are concerned.

With respect to the diatoms much of the work that has been done is limited to a very few wavelengths (Dutton and Manning, 1943; Wassink and Kersten, 1946; Mcleod and Kanwisher, 1962; and Bishop, 1967), or the experimental conditions are so specialized as to make the study useless for present purposes (Emerson and Rabinowitch, 1960). Potentially useful action spectra are available from the work of Tanada (1951), Mann and Myers (1968), and Iverson and Curl (1973), (figure III.8). The curves from the last two authors are quite similar but differ strongly from the Tanada curve. The Tanada curve is frequently referenced in the literature (Rabinowitch, 1951; Parsons and Takahashi, 1975; Steeman-Nielsen, 1975). Its most distinctive feature is the relatively flat high response in the 500-700 nannometer range. This high level response over such a broad range is rather surprising, since pigment absorption studies (Tanada, 1951; Margulies, 1970) show minimal light absorption between 500 and 625 nannometers. A flat response of this sort suggests the possibility that Tanada's light intensities were inadequately controlled and that saturating levels were employed. For this reason, the Tanada curve is rejected for present use.

With respect to the dinoflagellates, the only useful studies giving photosynthetic efficiencies over a broad range of wavelengths, and at fairly tight intervals, are those of Haxo (1960) for Gonyaulux polyedra, and of Halldal (1968) for symbiotic algae of the massive coral Favia sp. (figure III.9). The two curves are quite similar suggesting that they represent reasonable depictions of the dinoflagellate photosynthetic action spectrum.

In light of Steeman-Nielsens (1975) view that action spectrum differences between the diatoms and dinoflagellates should not be

Figure III.8. Photosynthetic action spectra for diatoms. Curve A based on Tanda (1951). Curve B based on Mann and Meyers (1968). Curve C based on Iverson and Curl (1973).

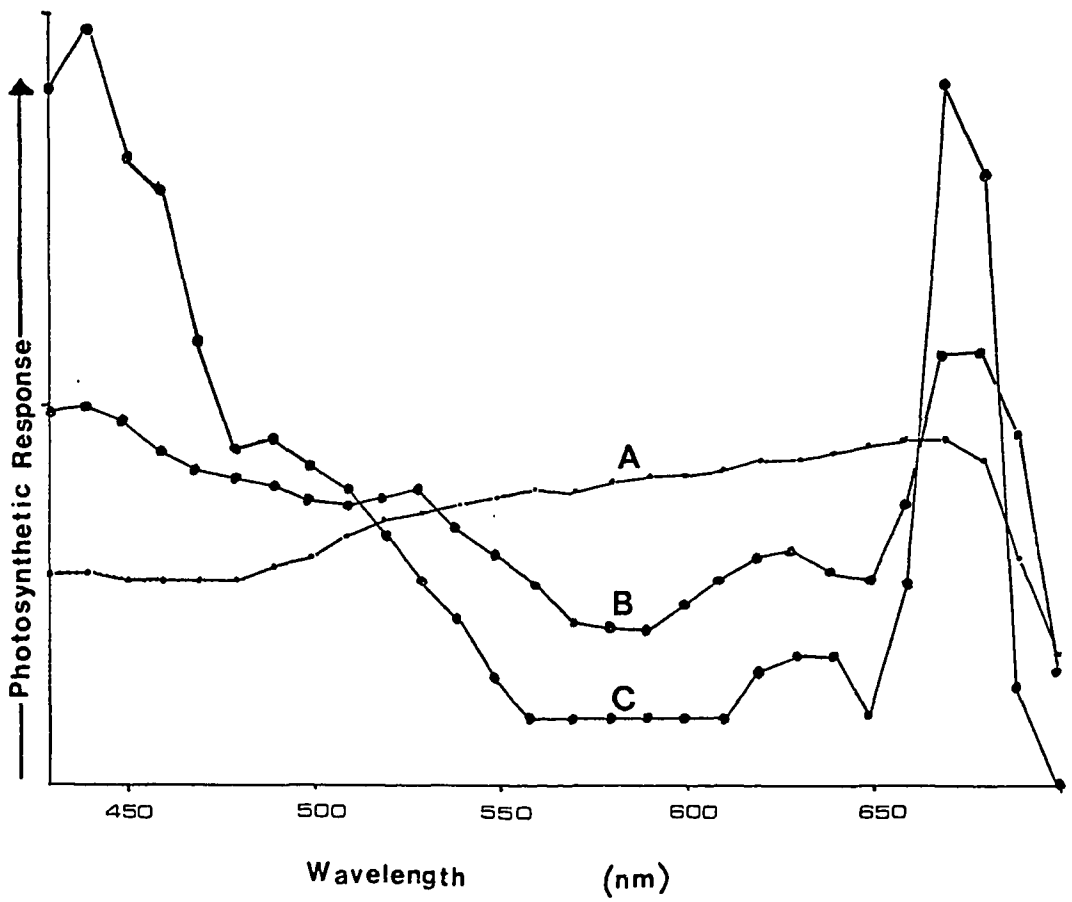

Figure III.9. Photosynthetic action spectra for dinoflagellates. Curve A based on Haxo (1960). Curve B based on Halldal (1968).

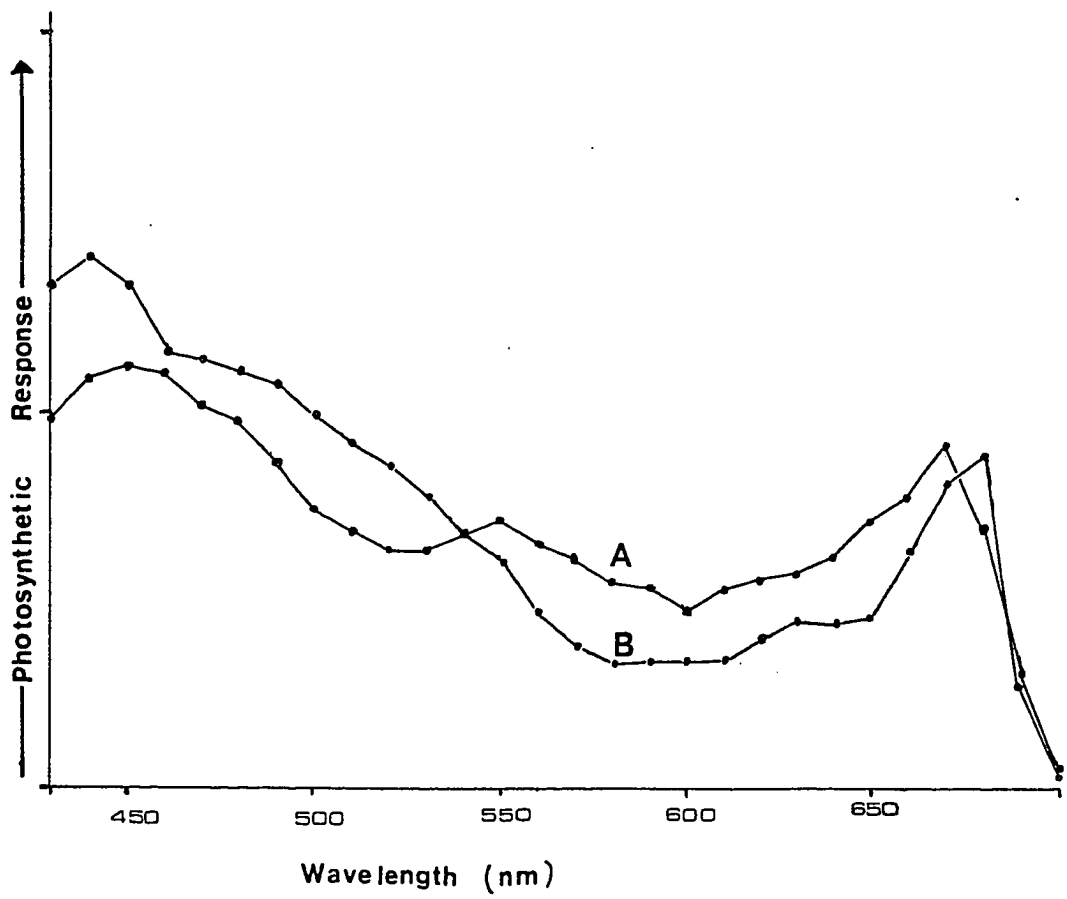

ecologically significant, extreme cases have been concentrated upon for comparative purposes. For this reason the diatom action spectrum obtained by Iverson and Curl (1973) and dinoflagellate action spectrum obtained by Halldal (1968) have been employed. These two curves are directly compared in figure III.10. It must be noted that the only information available on photosynthesis in the near ultraviolet range is that given by Halldal for the Favia symbionts. Iverson and Curl's data has been extended into this same range by normalization with Hallda's near-ultra-violet data.

Light Curve Constants

The constants $P_{m\lambda}$, $I_{k\lambda}$, I_i, and I_t are critical to defining the shape of the photosynthetic light intensity curve. Since it is not necessary to determine absolute carbon synthesis, the saturated rate of synthesis can be set equal to unity. The parameter $I_{k\lambda}$ is determined by equation 4.11, which depends in part on the parameter I_{kr}. This latter parameter is here derived from Pickett and Myers data, and is taken equal to .0287 $cal.cm^{-2}$ $min.^{-1}$, with 680 nm being the reference wavelength.

While Ryther's data suggests that I_r is division specific, it is desirable to employ the same value for diatoms as for the dinoflagellates. Otherwise, the effects due to differences in action spectrum could not be isolated from effects due to differences in light intensity requirements. At any rate, recent studies (Dunstan, 1973, MacIsaac, 1978) suggest that there are no real differences in the light intensity requirements for these two groups.

With respect to the photoinhibitory parameters, selection of specific values is somewhat arbitrary. While division specific values

Figure III.10. Photosynthetic action spectra for diatoms and dinoflagellates as used in the present study. Photosynthetic response measured in relative units. Data for diatoms based on Iverson and Curl (1973). Data for dinoflagellates based on Halldal (1968). Photosynthetic responses for diatoms, at wavelengths less than 400, based on Halldal's (1968) dinoflagellate data, equal area normalized to Iverson and Curl's (1973) data.

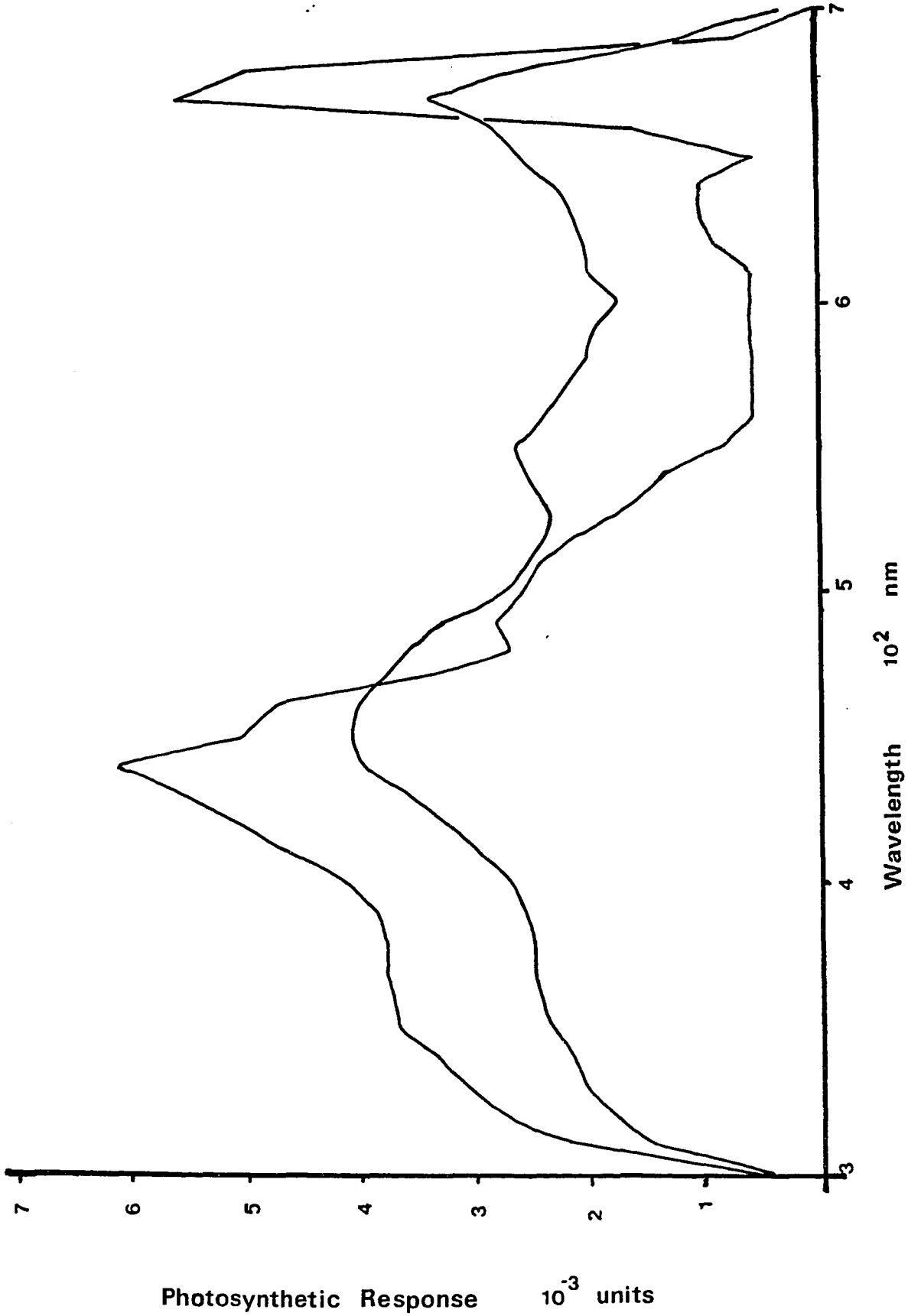

for I_k and I_m are known, or at least accepted in the literature (Ryther, 1956; but compare Dunstan, 1970; and MacIsaac, 1978) the comparable values for I_i and I_t are not known. From the data of Kok (1956), it would appear the initiation of photoinhibition is somewhat dependent on environmental parameters. For present purposes it will be assumed that photoinhibition is initiated at $I_i = 2\ I_k$, and that it is complete by $I_t = 3\ I_k$.

Action Spectrum Constancy

Photosynthetic action spectra are not entirely constant even within the same species, let alone the same division. There is ample evidence in the literature supporting the view that certain chromomutagenic processes exist and influence photosynthesis. It is known, for example, that the pigment concentration of a species is subject to change dependent on the overall light intensity to which it is exposed (Myers and Kratz, 1955; Brown et al., 1967; Jorgensen, 1969; Calabrese, 1972; Mandelli, 1972; and Calabrese and Felicini, 1973). This has obvious importance in governing the overall rate of photosynthesis. More critical are studies which have shown that pigment composition itself is subject to some degree of variation depending upon maturation state, (Carreto and Catoggio, 1971) and light quality, (Brody and Emerson, 1959; Jones and Myers, 1965 ;Fork and Amesz, 1967; O'Quist, 1969; Kirk and Reade, 1970; Wallen and Geen, 1971a,b,c; Mandelli, 1972; Bennett and Bogorad, 1973; Guerin-Dumartrait et al., 1973; and Waaland et al., 1974). This is demonstrated by changes in both absorbance and action spectra. While there are numerous studies showing this qualitative effect, the degree of detail which they show is insufficient to justify attempting to correct action spectra according to prevailing light quality.

CHAPTER IV

RESULTS

Introduction

In order to evaluate the capabilities of the model with respect to the hypothesis being tested, a series of runs were executed. Each run represented a variation in perspective and/or parametric valuation. In the following sections these runs will be given in detail. These outputs fall into three major classifications: 1) atmospheric light regime, 2) hydrospheric light regime, and 3) biological responses.

Light Regime Responses

Atmospheric Light Regime

Solar Elevation. In terms of model capabilities the dominant factors controlling the atmospheric light regime are solar elevation and atmospheric aerosol load. Considering first the influence of solar elevation, figure IV-1 shows the global monochromatic irradiances predicted by the model for a moderate aerosol load ($\beta = 0.1$), at various solar altitudes. Superimposed (open circles) are monochromatic global irradiances at selected wavelengths taken from Kimball's (1924) spectral distributions at comparable altitudes, normalized to 500 nm. Concordance between the two sets of data is quite striking. The relatively greater departure observed at low solar altitudes is considered to be within the range of environmental variability.

Figure IV.1. Global monochromatic irradiances predicted by the model for a moderate aerosol load ($\beta = 0.1$) at solar altitudes of 90° and 9°. Data from Kimball (1924) is superimposed.

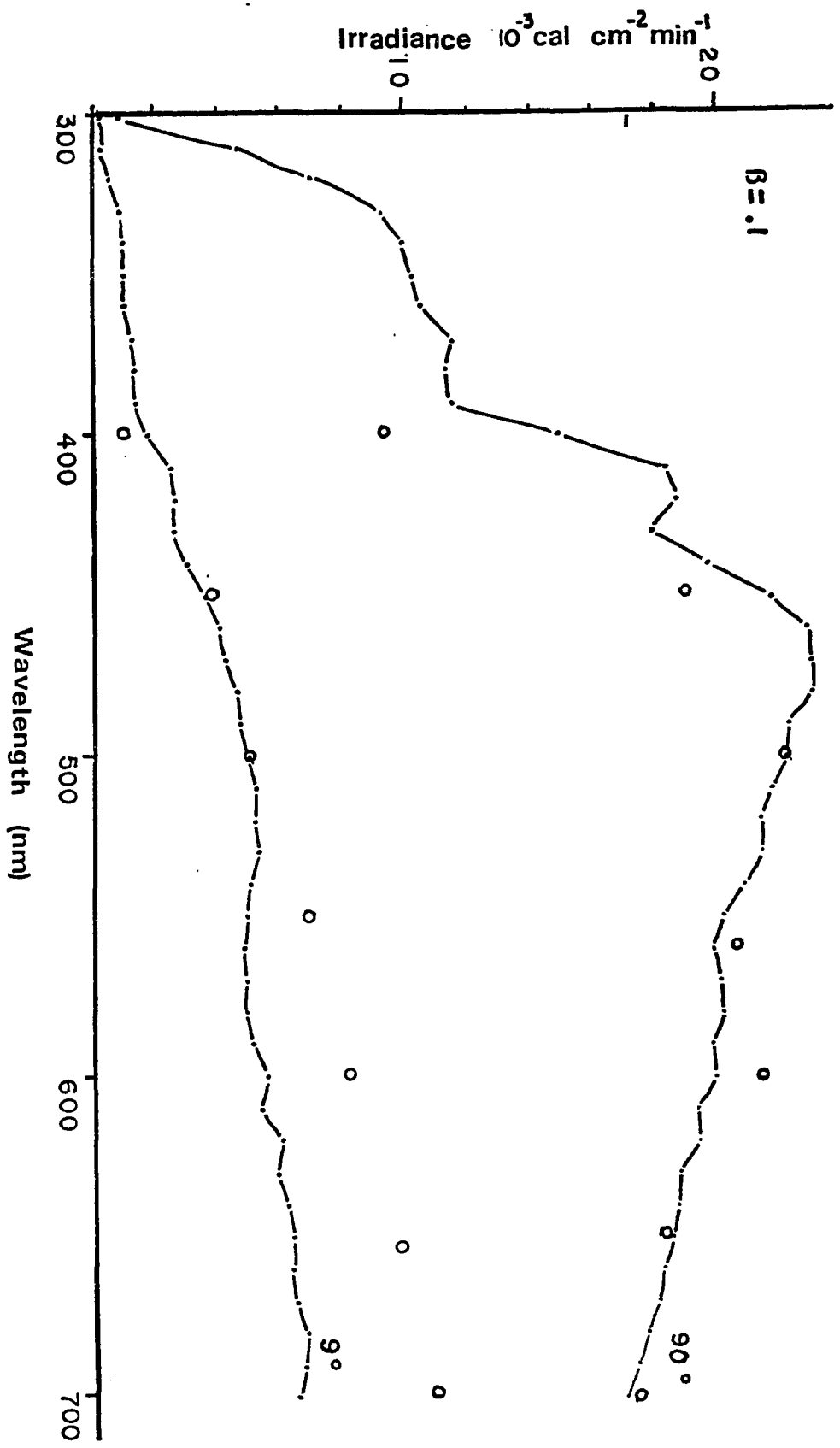

The same two dominant trends are observed in Kimball's real world data, and in the model's predictions:

- o Global monochromatic irradiance decreases with solar altitude.
- o At low altitudes the peak in the spectral distribution shifts toward the red end of the spectrum.

Aerosol Load. Figure IV-2 shows the influence of variation in atmospheric aerosol load on the light regime, as predicted by the model. Two generalizations can be made on the basis of this output:

- o Global monochromatic irradiance decreases with increasing aerosol load.
- o This effect is relatively greater above than below 400 mm.

Direct comparison of the model output with real world data is difficult because of the absence of real world measurements correlated with Angstrom turbidity measures. However, comparison of Kimball's data (1924) for clear and hazy day conditions (Table IV-1) reveals the same two trends as outlined in the previous paragraph for the computer model results.

Hydrospheric Light Regime

Hydrospheric light regime outputs generated by the model can be influenced through variation in the following factors:

Figure IV.2. Influence of aerosol load on atmospheric light regime. A value of $\beta = 0.0$ indicates absence of aerosols from the atmosphere. A value of $\beta = .1$ indicates a moderately turbid atmosphere.

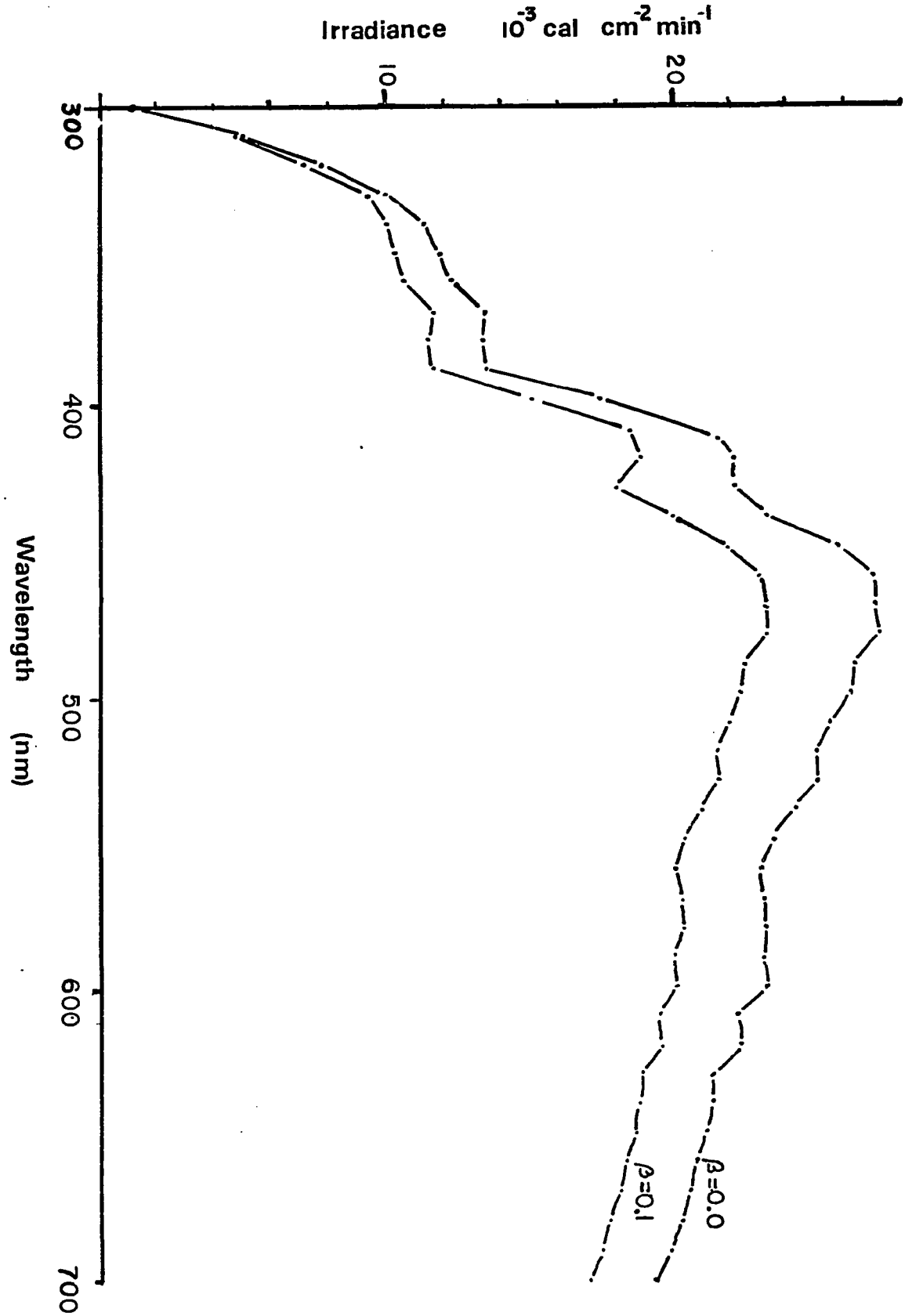

Wavelength (nm)	14 May Sky Hazy	Average Cloudless Sky	15 February Sky Clear
397	123	153	165
413	165	185	205
431	173	186	187
452	176	206	210
475	193	216	238
503	199	217	225
535	189	205	202
556	200	200	200
574	192	200	197
591	194	201	200
624	192	202	191
653	187	194	189
686	181	192	177
720	166	177	160

Table IV-1. Atmospheric light (relative energy units) under high, medium, and low turbidity conditions, according to Kimball (1924).

- o atmospheric input
- o depth in the water column

Other potentially relevant factors (such as sea state, optical water type, water column structure, and so forth) are obviated by the previously discussed assumptions. Some factors (such as sun angle and atmospheric aerosol load) indirectly influence hydrospheric light regime through their influence on the atmospheric light regime. For present purposes it is convenient to assume atmospheric light regime generated with the solar altitude = 90°, and a moderate aerosol loading factor (β = .1). The hydrospheric light regime at varying depths associated with these conditions, as generated by the model, is shown in figure IV-3. The following trends with increasing depth are to be noted:

- o an exponential reduction in monochromatic light intensity
- o the light becomes progressively more monochromatic, centering on the 410 to 490 mm range.

Comparison of the results generated by the model with real world observations (figure IV-4) for selected depths shows good agreement between the model and the real world.

Biological Response

Time-Depth Incrementation

In computing the total daily rate of carbon synthesis over the depth of the water column and the course of the day, a finite difference

Figure IV.3. Hydrospheric light regime as a function of depth. (Depths in meters).

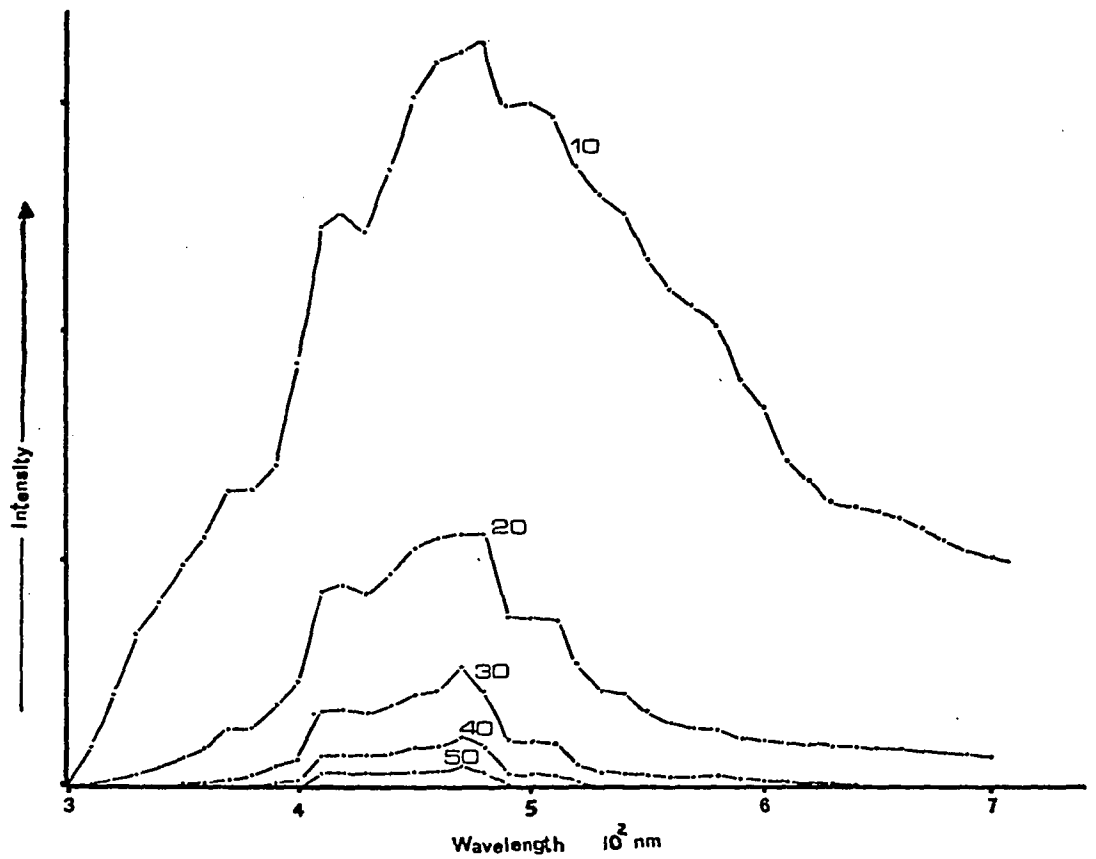

Figure IV.4. Hydrospheric light regime as a function of depth. Based on Jerlov 1968.

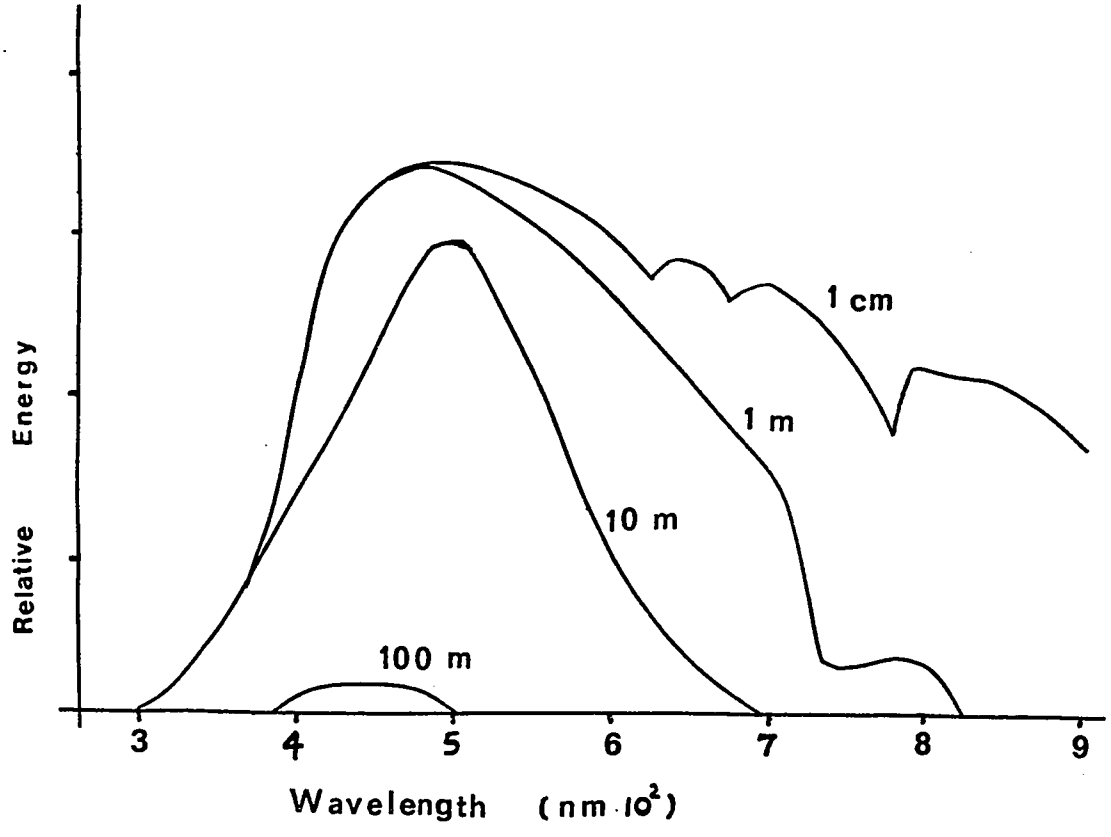

scheme is employed in the model. This involves the determination of a rate of carbon synthesis at specified depth and time intervals, the determination of an average rate for each depth-time volume, and a determination of the overall rate by summation over depth and time. The absolute values obtained in this manner are sensitive to the increment size at which the initial calculations are made. In general, greater accuracy is to be obtained with the smallest step sizes; however, decreasing step size increases computation time. There is, then, a tradeoff between accuracy and cost-effectiveness.

With respect to the selection of an appropriate time increment step, initial runs were performed dividing the day into 10-step increments. As a test a carbon synthesis rate for the day was computed on 1 January at the equator, first with a 10-step increment, then with a 20-step increment. No differences were found at the 0.00001 level, despite an observed doubling of computation time. For this reason a 1/10-day increment was selected as standard for all further computations.

A similar analysis was performed for varying depth step incrementation. The results of this analysis are presented in figure IV-5. It is apparent that depth increment size does strongly influence carbon synthesis rates generated by the model. A step size of 10 meters was found to be a practical limit below which computer time became excessive. For this reason a 10-meter increment was accepted as standard.

Figure IV.5. Photosynthetic response as a function of depth step size employed in the model.

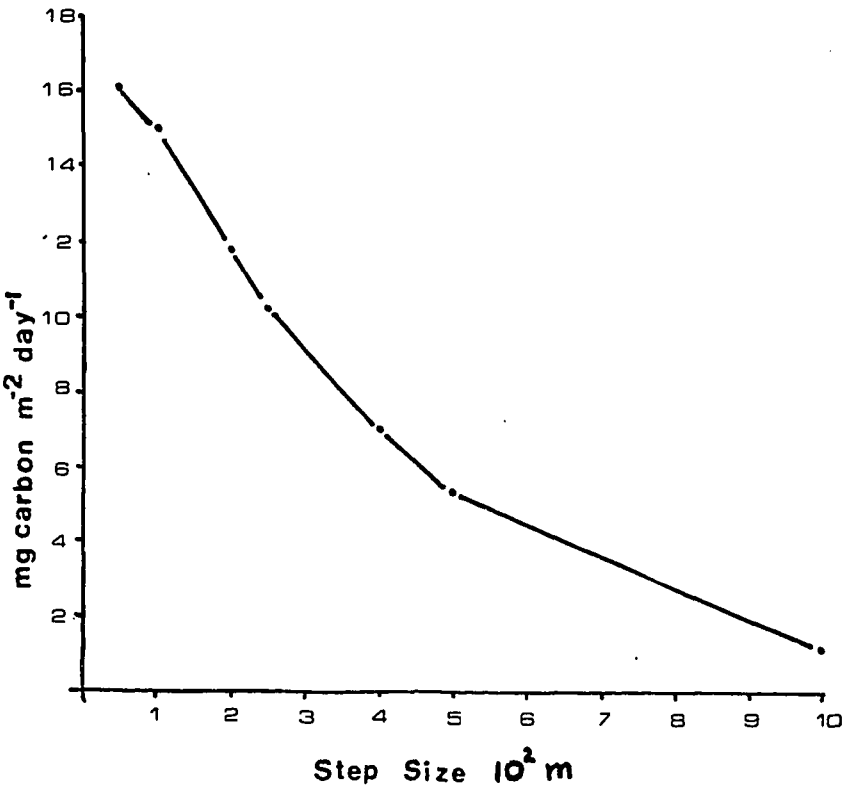

Depth-Altitude Dependence

Figure IV-6 depicts the results of a run in which the ratio of diatom to dinoflagellate carbon synthesis (Ψ) was determined as a function of a depth in the water column and solar altitude. A moderately turbid atmosphere was assumed ($\beta = 0.1$). The I_k values were taken to be constant, with action spectra division specific. The following trends are apparent:

- A strong shift in Ψ favoring the diatoms with increasing depth.
- This shift amounts to 11% to 22% comparing the 10 m and 200 m levels, depending upon solar altitude.
- The sharpest fluctuations occur over most of the water column when the sun is between zero and 10 degrees above the horizon.
- In the upper 30 meters the dinoflagellates are favored when the sun is between roughly 5 and 30 degrees above the horizon.
- At deeper depths there is a progressive shift toward increased dinoflagellate carbon synthesis when the sun is above 30 degrees altitude.

Season-Latitude Dependence

Figure IV-7 shows the results of a computer run generating Ψ ratio at various latitudes over the course of the first half of the year. (Data for the second half of the year is simply reflexive.) In this run the I_k values for the diatoms and dinoflagellates are assumed to be constant; that is, it is assumed that they have the same light intensity response pattern. The respective action spectra are assumed to correspond to the extreme cases previously detailed; that is, the chromatic responses of the two groups are as diverse as can be justified. A moderately turbid atmosphere ($\beta = 0.1$) is assumed. The following features are worth noting:

Figure IV.6. The ratio (ψ) of dinoflagellate to diatom carbon synthesis as a function of depth and solar altitude.

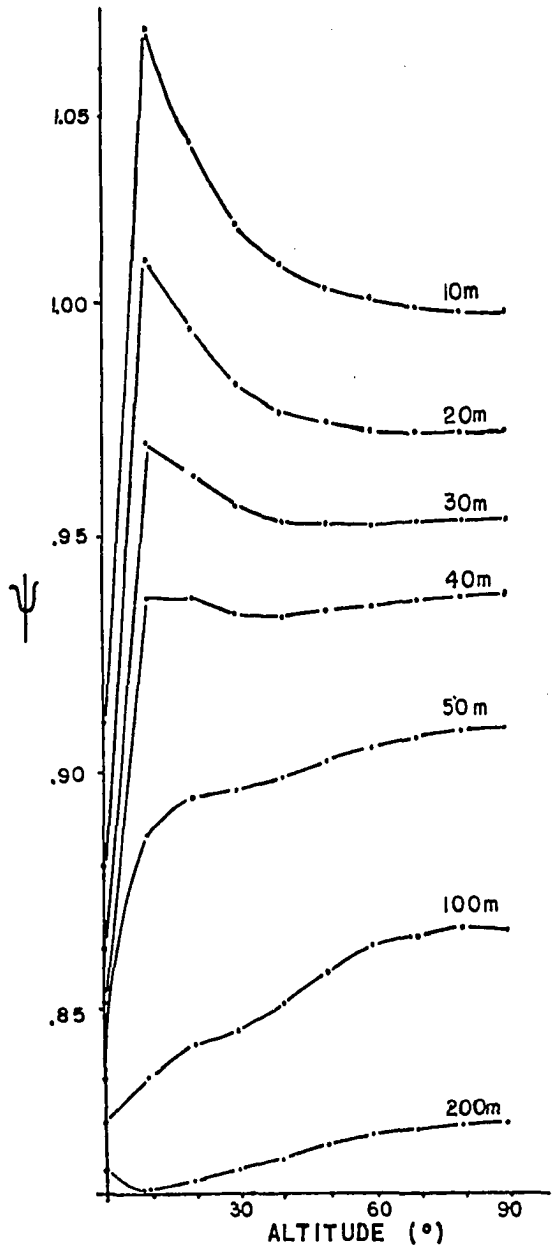

Figure IV.7. The ratio (ψ) of dinoflagellate to diatom carbon synthesis as a function of latitude and season, at a moderate (β = 0.1) aerosol load. Day number 91 = 1 January; Day number 281 = 1 July.

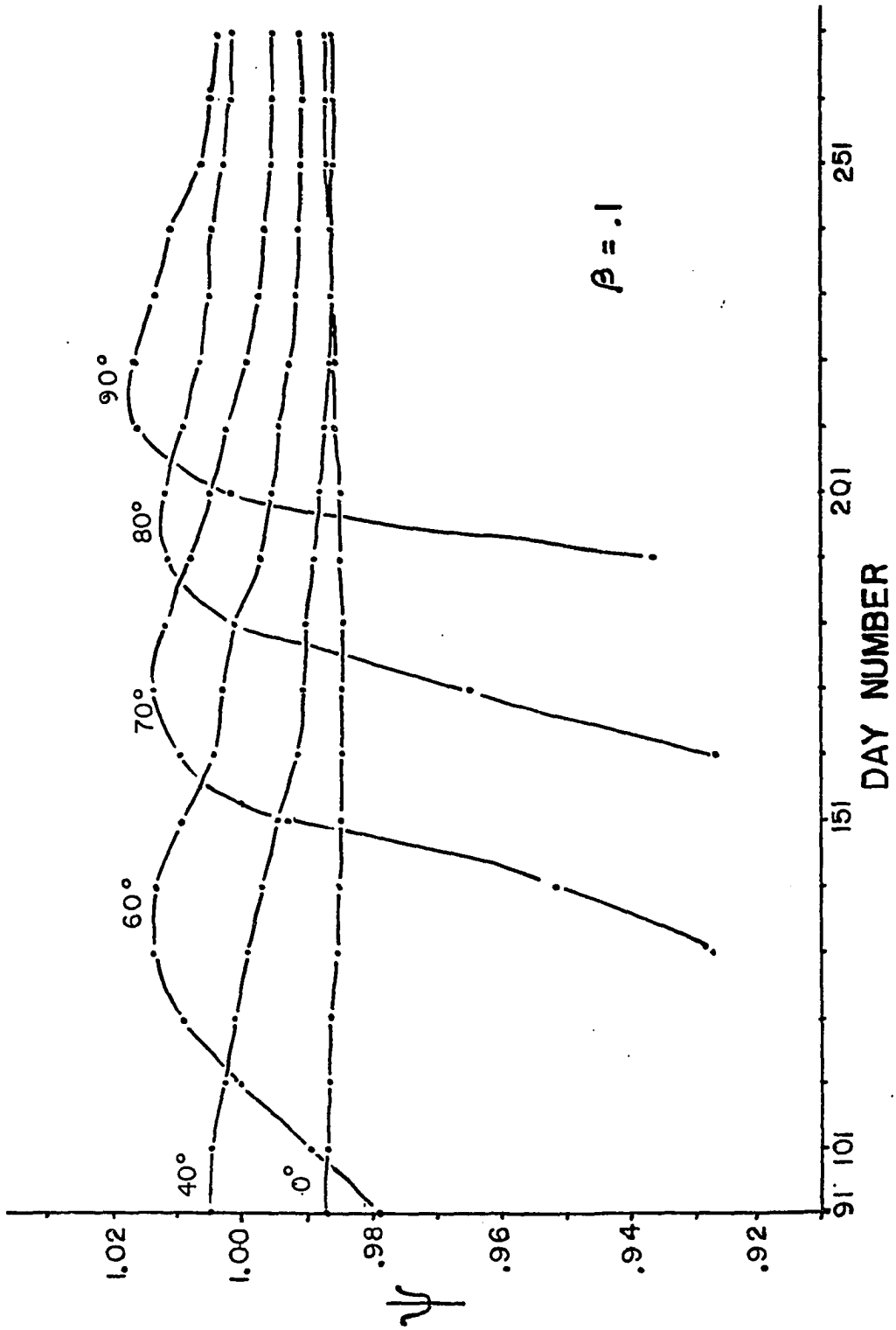

- The shift toward dinoflagellates occurs later in the year with increasing latitude.
- Near the equator the ψ ratio is relatively constant over the course of the year.
- The largest fluctuations in the ψ ratio occur at the higher latitudes over a short period in the spring and fall.
- At high latitudes the rate of carbon synthesis favors the diatoms during the spring and fall, and the dinoflagellates during the summer.
- The absolute magnitude of the fluctuations are small, being never greater than 10%.

Similar runs were performed at other turbidity levels. Figure IV-8 shows the responses for a very clean atmosphere (no aerosols, $\beta = 0.0$, i. e., a Rayleigh atmosphere). Figure IV-9 shows the response for a very turbid atmosphere (extreme aerosol loading, $\beta = 0.2$). These two cases represent what are probably unrealistic extremes; they do show, nonetheless, the profound influence which turbidity exerts on marine photosynthetic responses. Figure IV-10 is instructive in this regard, showing the influence of turbidity on the absolute daily diatom carbon synthesis achieved under various atmospheric turbidities. As is readily apparent, turbidity plays a major role in governing absolute carbon synthesis. In the instance illustrated by the data in figure IV-10 (corresponding to a mid-year date) the reduction in diatom carbon synthesis between a very clear and a highly turbid atmosphere amounts to as much as 45%.

From the perspective of season-latitude dependence, another run was performed utilizing identical system parameters, excepting that the I_k values were taken as consonant with Ryther's (1956) curves, and the

Figure IV.8. The ratio (ψ) of dinoflagellate to diatom carbon synthesis as a function of latitude and season at a low (β = 0.0) aerosol load.

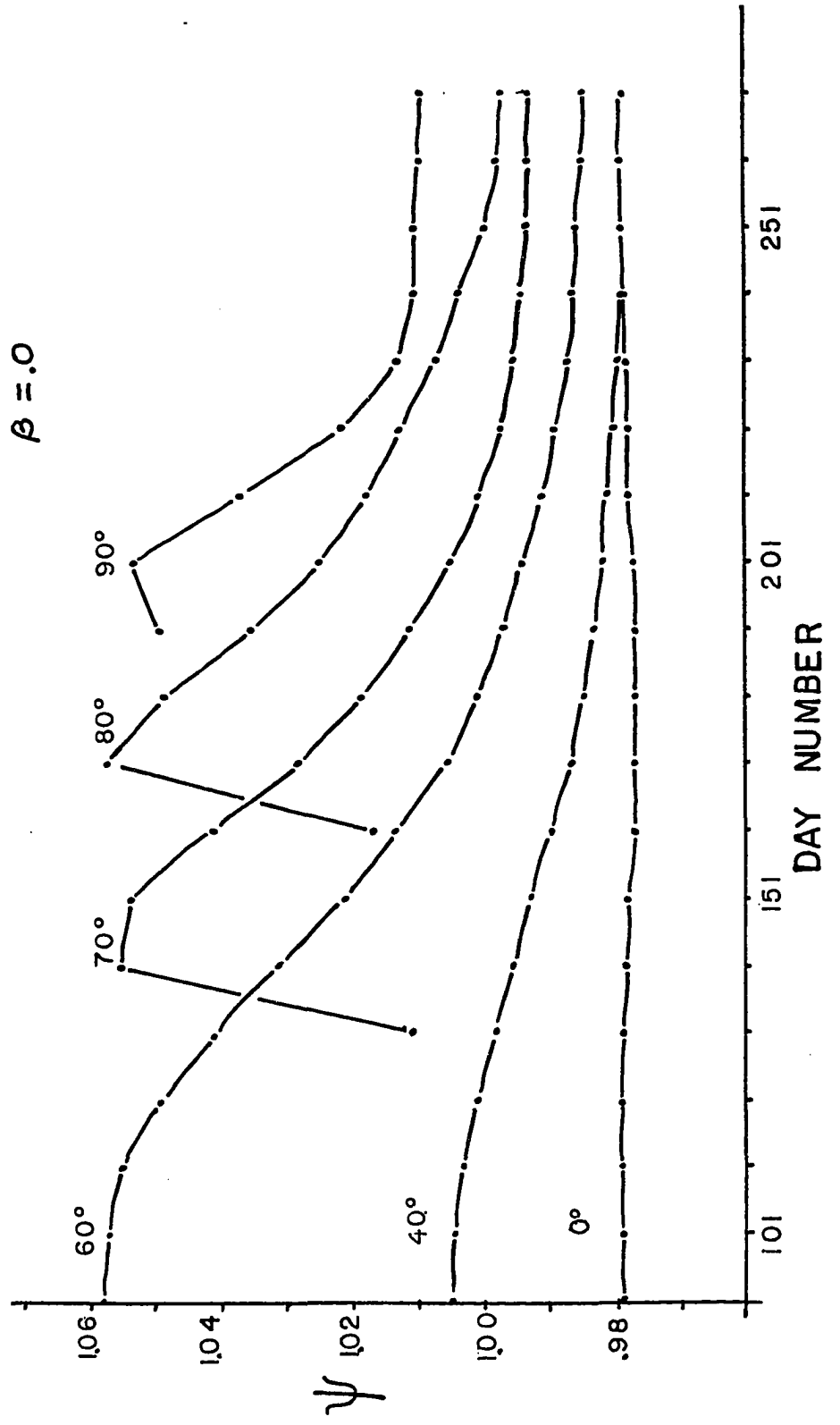

Figure IV.9. The ratio (ψ) of dinoflagellate to diatom carbon synthesis as a function of latitude and season at a high (β = 0.2) aerosol load.

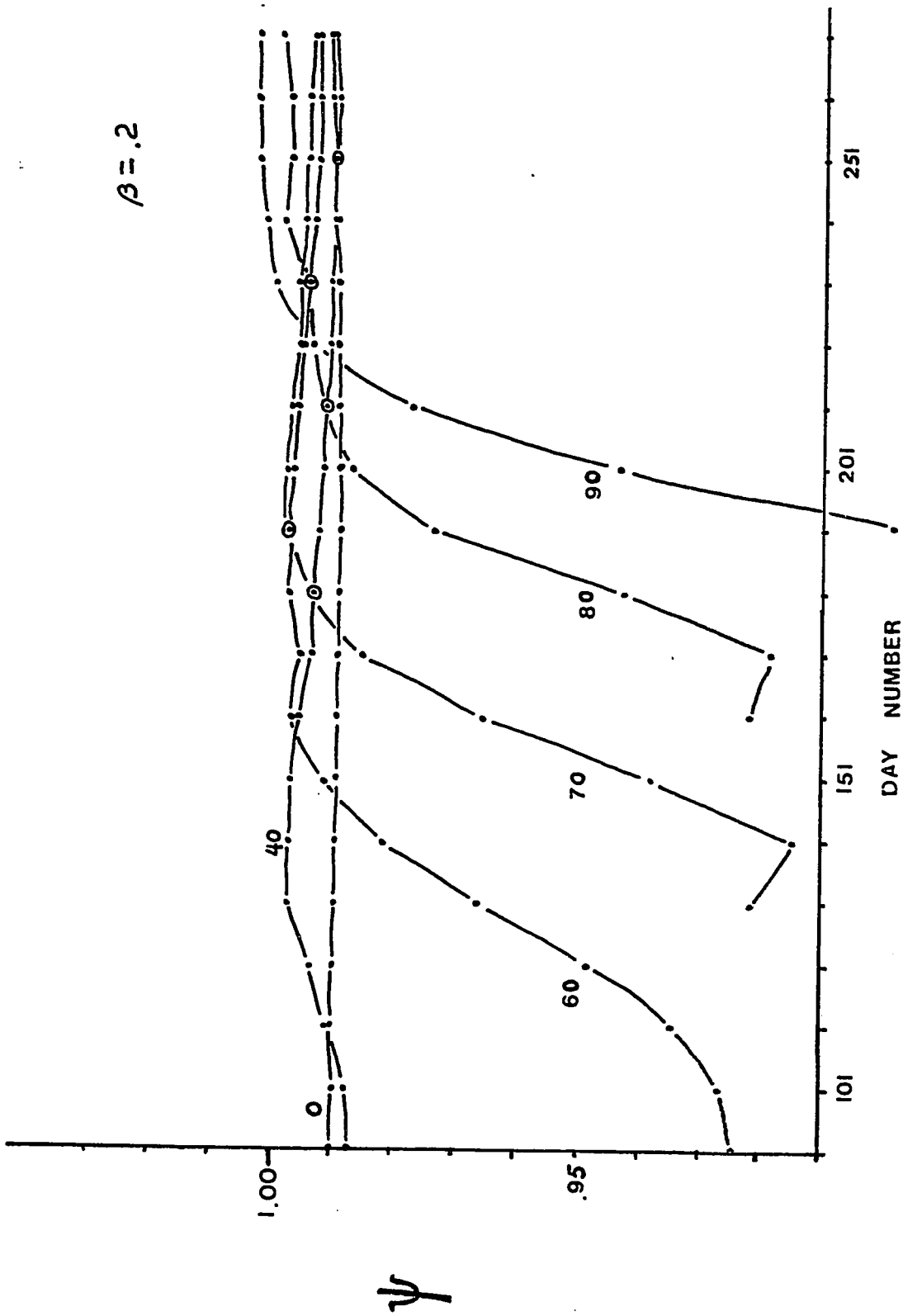

Figure IV.10. Daily carbon synthesis as a function of latitude at low (β = .0), medium (β = .1), and high (β = .2) aerosol loads.

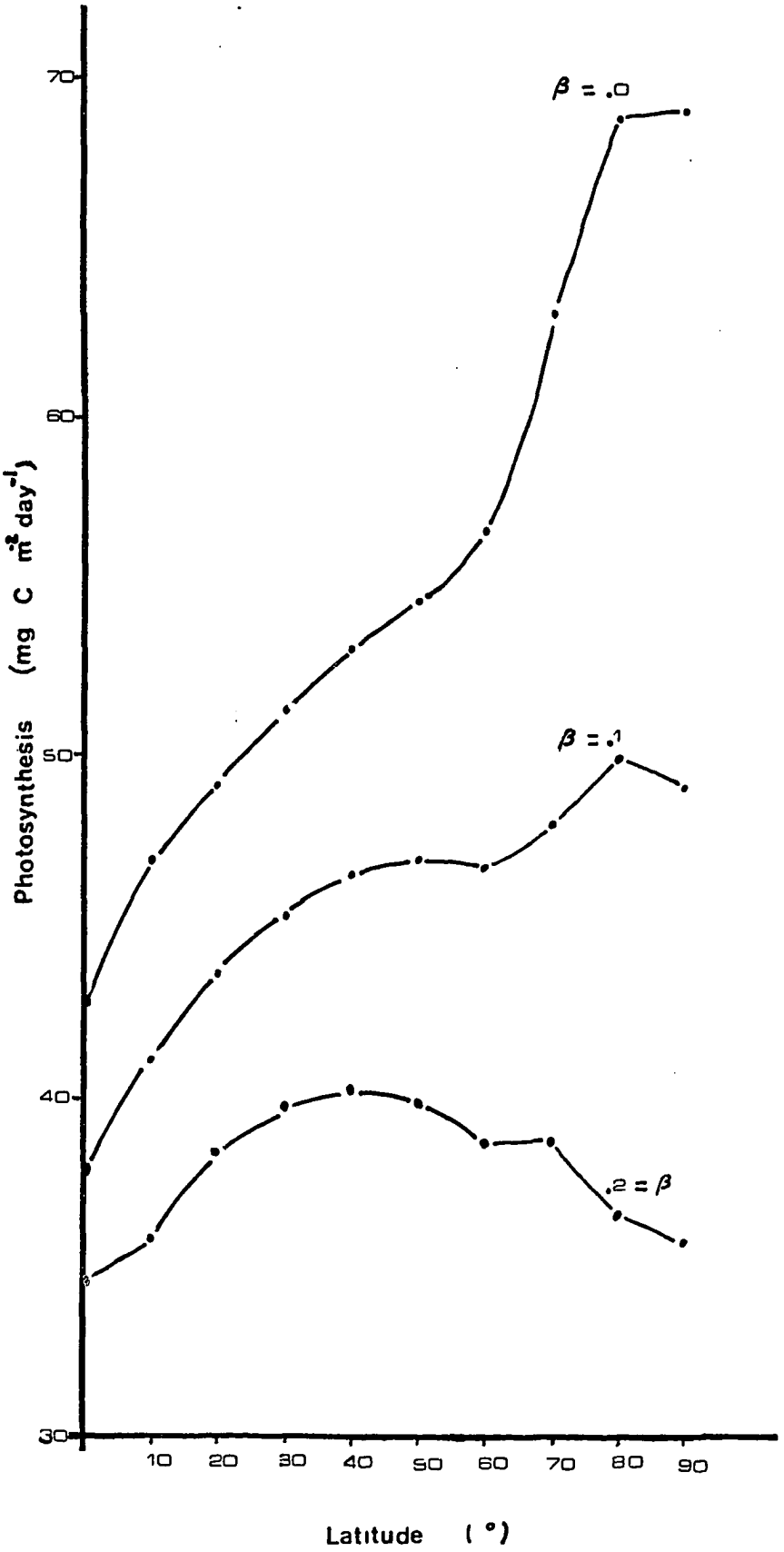

division specific action spectra were assumed to be identical to each other (i.e., that of the diatoms). Under worst case conditions (very clear atmosphere, $\beta = 0.0$) the variation in the ψ ratio amounted to no more than 0.64%. This compares with a worst case variability of 8.41% for runs with constant I_k and variable action spectra.

Carbon Synthesis Depth-Altitude Dependence

In its present form the model assumes a unit value for the maximum rate of carbon synthesis. In reality, this parameter is a function including nutrient state, temperature, salinity, and other factors. In consequence it is not possible to employ the model to determine absolute carbon synthesis for comparison with real world observations. It is possible, however, to determine the relative rates of carbon synthesis with respect to depth in the water column, and time of day/solar altitude. Results of model runs generating this data are shown in figures IV-11 and IV-12. A moderately turbid atmosphere ($\beta = 0.1$) was assumed. Only diatom carbon synthesis is shown; dinoflagellate synthesis is very similar.

Several trends are noteworthy:

- Carbon synthesis in the surface waters reaches a peak at relatively low sun angles, and is severely depressed when the sun is near the vertical.
- At increasing depth the peak in carbon synthesis is achieved at progressively greater solar altitudes; below 20 to 30 meters no depression is evidenced.
- Apart from the depression in the surface waters at large solar altitudes, carbon synthesis decays exponentially with depth.

These trends are qualitatively consonant with real world observations on carbon synthesis in the ocean.

Figure IV.11. Photosynthetic response as a function of solar altitude and depth (in meters) in the water column. Insert shows comparable data from Ryther (1957), for depths where the light intensity was equivalent to a certain fraction of the surface intensity, Io : A = Io, B = 50% Io, C = 25% Io, D = 10% Io, E = 1% Io.

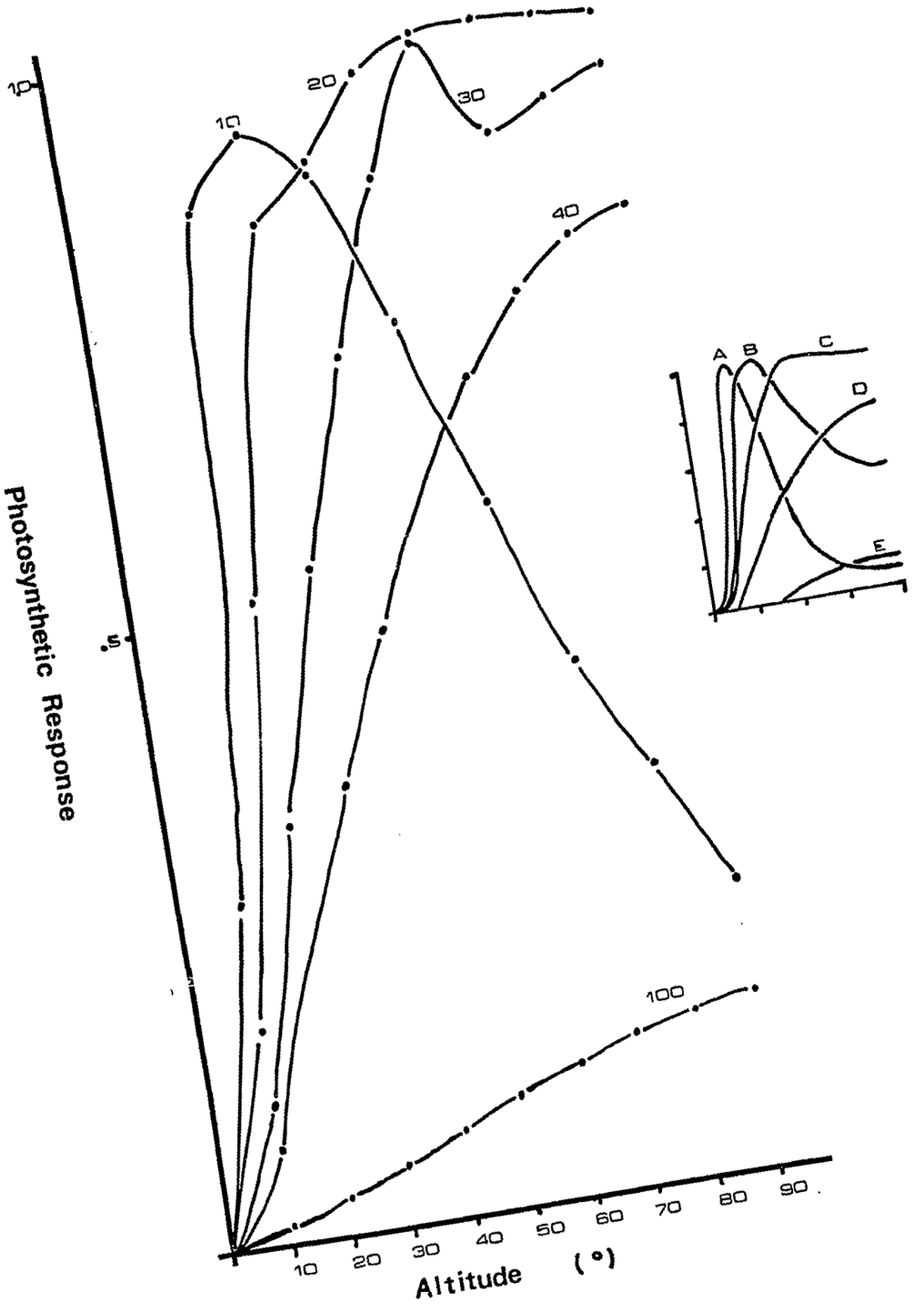

Figure IV.12. Photosynthetic response at a solar altitude of 90° as a function of depth (in meters). Solid line = model results. Dashed line based on data from Ryther (1957) with arbitrary depth units.

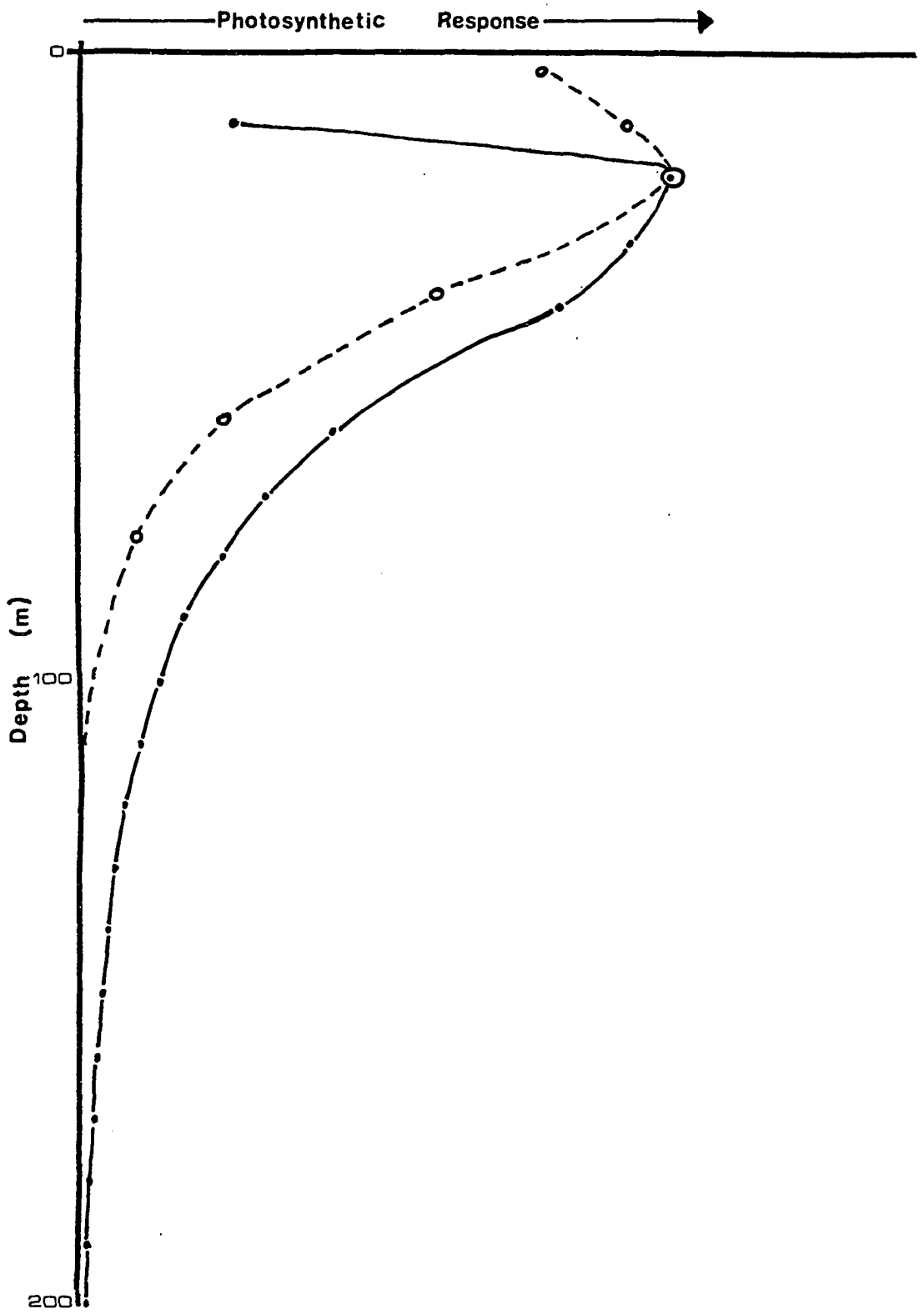

CHAPTER V

DISCUSSION

The results of the model runs detailed in the previous chapter strongly suggest that light regime, and particularly spectral composition, exerts an influence on the relative abilities of the diatoms and dinoflagellates to synthesize carbon. Assuming that the ratio between net and gross carbon synthesis is the same for both groups and other factors are equal, it would seem that such differences in synthesis rates would be directly reflected in the relative sizes of the respective population carbon pools. This being the case two questions arise: first, are the observed differences in synthesis rates sufficient to exert a significant ecological effect; and second, if so, to what extent could these differences account for variations in the donoflagellate/diatom ratio in the real world?

In response to the first question, it should be borne in mind that it is not the specific value of the dinoflagellate/diatom carbon synthesis ratio (ψ) which is significant, but the changes in that ratio through time and space. This is because photosynthetic action spectrum is only one of several factors which in the real world must influence ψ; since these factors are unaccounted for in the model, it is useless to discuss absolute values of ψ predicted by the model in assessing real-world processes. However, if these other factors are held constant through time and space, and are independent of action spectrum, the fluctuations in ψ predicted by the model can be considered meaningful.

On the basis of the above, it is to be noted that the magnitude of fluctuation of ψ is relatively slight under the circumstances examined in the present study. For the most part, these fluctuations were less than 10%, though under certain specialized circumstances differences of 25% were observed. Not all of the carbon synthesized can be directly converted into upgrowth of the population; a certain fraction must be expended in metabolic processes and lost through predation. If net carbon synthesis is set at 50% of the gross, then the model predicted fluctuations in ψ are typically less than 5%, and never much more than 12%. Even so, such slight differences are probably ecologically significant, as their effect is cumulative and should follow the exponential growth model:

$$N_t = N_o e^{rt} \qquad 5.1$$

where N_o is the initial carbon pool, N_t is the pool at time t, and r is the rate of carbon synthesis. If the initial carbon pools for the dinoflagellates and diatoms are assumed equal, the respective gross synthesis rates are taken as $r_1 = 1.00$ and $r_2 = .95$ (5% difference), and the net rates are taken as $r_1 = .50$ and $r_2 = .475$, the difference in carbon pool size would amount to 50% after only 12.2 days. Thus, a relatively small step fluctuation in carbon synthesis rate can have magnified effect on carbon pools over a fairly short period of time.

It is thus seen that the relatively small differences in photosynthetic action spectrum exhibited by the diatoms and dinoflagellates are sufficient to impact significantly the relative sizes of the population carbon pools. This being the case, it is of interest to

consider the circumstances under which these differences might be expected to produce a successional effect. The operating assumption underlying the present study is that such effects could be expected to some degree wherever gradients in light regime were to be found. The model predicts variations in ψ in each of the four dimensions along which gradients in spectral composition were expected:

- Depth in the water column (vertical)
- Time of day (diurnal)
- Time of year (seasonal)
- Latitude (latitudinal)

The diurnal variations in ψ predicted by the model are especially strong, amounting to as much as 20% in the surface layers, and at least 5% as deep as 100 meters. If the cell division rates for the diatoms and dinoflagellates were very rapid (say 10 divisions per day) such differences in ψ might be expected to produce a diurnal successional pattern with diatoms dominating during the early morning and late evening, and dinoflagellates dominating during midday. However, the actual cell division rates are much slower than this (one or two per day), and this probably precludes a pattern of diurnal succession.

While a diurnal succession is unlikely, the predicted variation in ψ with time of day is sufficiently large to suggest that it cannot be without ecological significance. An interesting possibility is that the diurnal variation in ψ represents a temporal resource partitioning mechanism. By isolating peak demands of the two groups for limiting resource pools, the difference in response to spectral composition may reduce direct competition, thereby permitting continued coexistence.

Variations in ψ with respect to depth are perhaps even stronger than those observed with time of day, showing a maximum variation between 10 and 200 meters of over 22%. The minimum difference in ψ for these two levels is better than 10%, and 20% is typical. Such severe differences are potentially of great significance, particularly where vertical mixing is relatively slight. Under such conditions the communities of the upper and lower portions of the water column would be isolated and the cumulative effects of a ψ differential would be quickly realized. This being the case it would be expected that variations of ψ with depth would be of particular significance during the summer months. During the winter months, vertical exchange of water (and hence intermixing of the upper and lower communities) would obviate the effects induced by response to the light regime gradient. Given the relative isolation of the upper and lower communities it would appear that the sharp differential in ψ predicted by the model would result in the development of a near surface community, dominated by the dinoflagellates, and a deeper community dominated by diatoms. This circumstance is supported by findings suggesting that the diatoms in fact dominate at deeper depths than the dinoflagellates (e.g., Riley, 1957). This is precisely analogous to the well-known Green-Brown-Red algal sequence in the benthic littoral.

Seasonal and latitudinal changes in ψ are not as strong as those observed for time of day (solar elevation) and depth in the water column. At equatorial latitudes the annual fluctuation in ψ, as predicted by the model, is trivial ($<10^{-3}$%). This suggests that changes in light regime at the equator do not serve as a forcing function governing community composition. However, with increasing latitude the annual

fluctuations in ψ become progressively more severe, reaching 8% at 90°N. Further, not only are these changes stronger, they are progressively compressed into shorter and shorter periods of time. Thus, at 40°N the maximum fluctuation is 2% over 180 days, but at 90°N the fluctuation is 8% over 23 days. Setting gross rates at $r_1 = 1.00$ and $r_2 = .92$, with net rates $r_1 = .50$ and $r_2 = .46$, the overall effect on the community composition may be calculated by equation 5.1. When this is done, it is seen that there is a six-fold change in the relative sizes of the diatom and dinoflagellate carbon pools between 1 January and 1 July at 40°N. At 90°N there is only a 2-1/2-fold change, but this occurs over a 23-day period.

Under conditions of a moderately turbid atmosphere the seasonal ψ curves for mid and high latitudes are markedly saddle-shaped. This is very similar to the diurnal ψ curves for the upper reaches of the water column. The saddle slopes in each case coincide with conditions where the spectral composition of the atmospheric light regime is strongly shifted toward the red end of the spectrum. When the photosynthetic action spectra for the two groups of algae are compared, it is apparent that the diatoms are strongly favored at the far ends of the photosynthetically active range of radiation; that is, in the blue and red regions of the spectrum. During the course of the day as the sun rises higher in the sky the peak of the spectrum of the atmospheric light regime shifts from the red into the green, blue-green, and finally into the blue regions (figure V.1). This sequence is mimicked in the hydrospheric light regime, at least in the upper portions of the water column. It is therefore to be expected that as the sun rises toward its zenith the diatoms will at first be favored, then the dinoflagellates,

Figure V.1. Spectral distribution of the atmospheric light regime as a function of zenith angle.

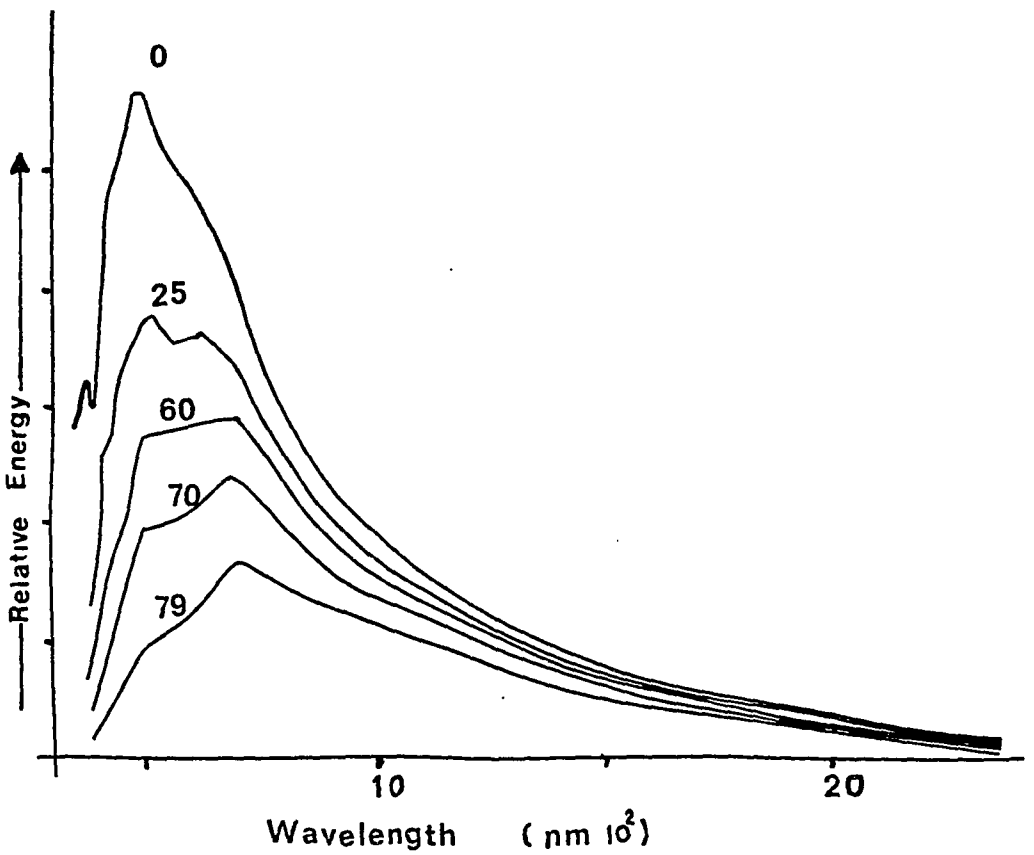

and finally the diatoms again. As the sun sets the reverse sequence would be expected. This obviously leads to the saddle-shaped ψ curves observed in the present modeling effort.

In terms of the seasonal ψ curves the same explanation must apply. However, in this case the relationship is more obscure, as solar elevation is not so strongly coupled with the time of year as with time of day. During the winter at high latitudes the sun never reaches as high an altitude as it does in the summer. Consequently, as the seasons progress from midwinter to midsummer the peak of the daily time averaged spectral composition shifts from the red into the green and finally into the blue regions in a manner exactly analogous to that observed during the course of a single day. Thus, at high latitudes a saddle-shaped seasonal ψ curve would be expected, as is, in fact, the case. At progressively lower latitudes the red peak in the spectrum would be expected to occur at progressively earlier dates. This would produce a broader "saddle" at the lower latitudes. At very low latitudes a red peak in the daily time averaged spectrum would not be expected at any time during the year, as the sun is generally high in the sky over most of the day. In fact, at equatorial latitudes little seasonal variation in the daily time averaged spectrum would be expected, so that the seasonal ψ curve should be flat. This agrees with the model results. At temperate latitudes (ca. 40°) an intermediate situation should prevail. The sun would never be low in the sky for a sufficiently protracted period so as to produce a well defined peak in the red; yet there would be some degree of seasonal change in the position of the peak, shifting between the green and blue regions. For this reason, a midwinter diatom preference might not be expected; rather, a midwinter

preference for dinoflagellates could be anticipated. This again agrees with model results.

While model results with respect to latitudinal patterns of seasonal succession are understandable in terms of the photosynthetic capabilities of the two groups and seasonal changes in light regime, the correspondence with real-world observations is not consistently good. At equatorial latitudes algal seasonality is relatively slight (Zaneveld, personal communication). This agrees with expectations and model results. Similarly, the winter dominance of diatoms at high latitudes agrees with expectations and model results. The fact that shift toward favoring dinoflagellates (cessation of the winter-spring diatom bloom) occurs at progressively later dates with increasing latitude agrees with real world results. Certainly, we know that the winter/spring bloom is delayed at higher latitudes (January in the Chesapeake Bay, February in Narragansett Bay, April-May in the sub-Arctic, and June in the Arctic, Bogorov 1956). However, the model implication that dinoflagellates should dominate the phytoplankton community at intermediate latitudes, while conforming with expectations based on action spectra and light regime patterns, is not supported by real-world observations. Rather, everywhere that seasonal patterns have been reported diatoms dominate the winter months and are replaced by dinoflagellates in the summer months.

This mid latitude discrepency between real-world conditions on the one hand, and theoretical expectations and model results on the other, is probably of minor significance. The mid-winter fluctuation in ψ is relatively slight (2%) at mid latitudes compared with that observed at 90°N (10%). Such a slight fluctuation could be masked by the effects of

non photic factors (such as division specific differences in nutrient requirements or temperature/salinity preferences). If this is the case the "discrepancy" is real, reflecting an unobservable real-world phenomenon. On the other hand, it is possible that the discrepancy is an artifact generated by certain assumptions in the model construction and execution. Of particular interest in this regard is the possibility that some of the atmospheric and hydrospheric light regime variables were assigned inappropriate values. Figure IV-9 depicts the seasonal ψ curves for a highly turbid (β = .200) atmosphere. Under these conditions the previously noted discrepancy is completely eliminated. While an atmospheric turbidity of this magnitude is unrealistic, these results point up the fact that atmospheric conditions play a significant role in defining ψ. Since the β (aerosol load) parameter varies in nature as a function of latitude (Angstrom 1961) it is possible that this variability had been accounted for in the model, the discrepancy would not have been observed.

When Figure IV-7 is examined in terms of latitudinal trends in ψ a similar discrepency between model results on real-world observations arises. Specifically, as a general trend on any given date ψ increases from the equator toward the poles. That is, the dinoflagellates tend to be favored with increasing latitude. (This is shown more clearly in figure V-2 in which the data for IV-7 has been replotted with latitude as the ordinate instead of time of year). This is at variance with real-world conditions where diatoms seem to be favored with increasing latitude (Moore 1966). However, the magnitude of the fluctuation in the latitudinal ψ curves is generally small, seldom exceeding 3%. While a 3% variation in daily carbon synthesis might be significant in itself,

Figure V.2. Variation in the ratio (ψ) of dinoflagellate to diatom carbon synthesis as a function of latitude and day of the year. Day number 91 = 1 January. Day number 271 = 1 July.

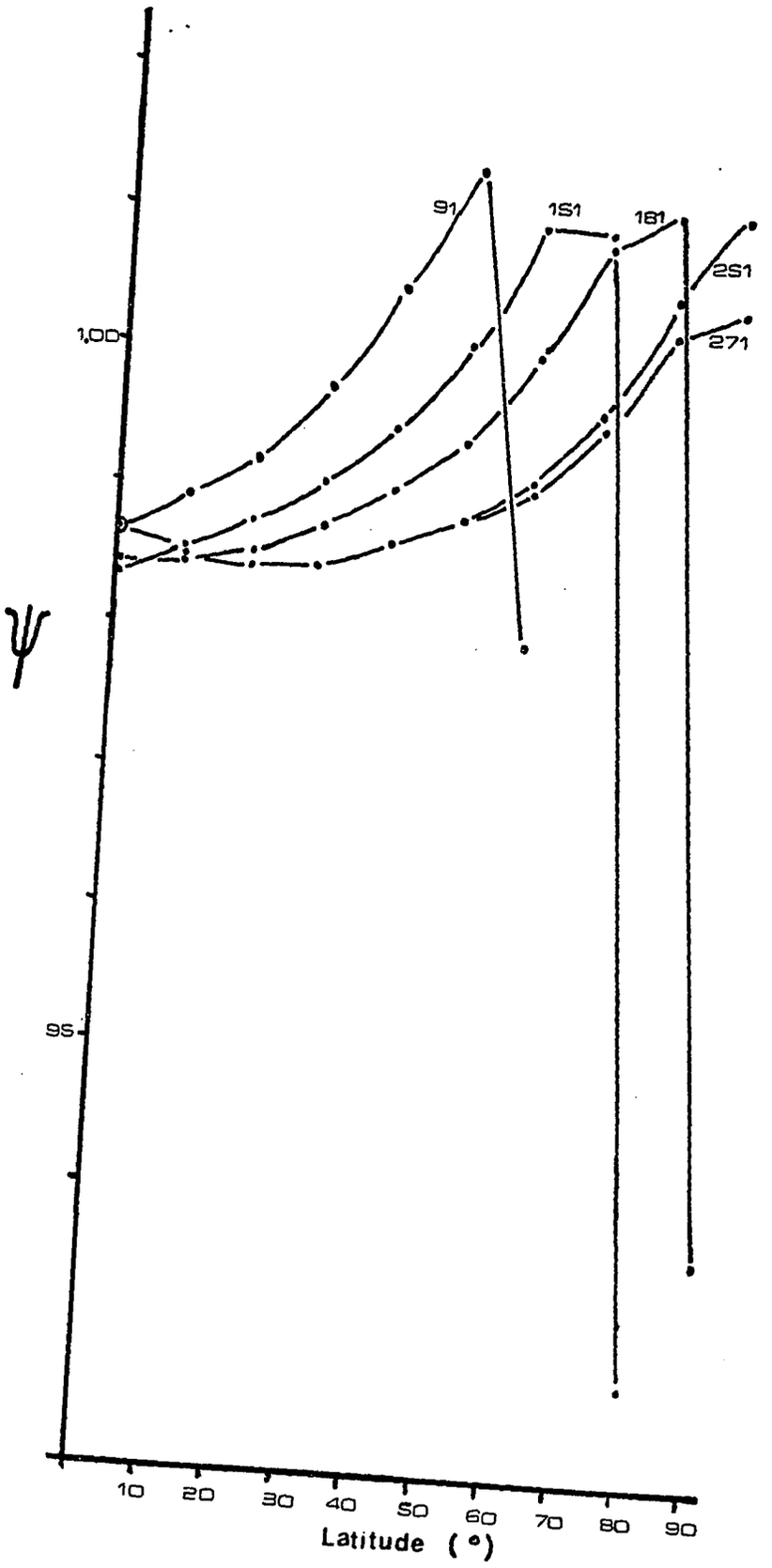

it is again likely, as discussed above, that other factors could mask such a fluctuation. On the whole, it would seem that changes in spectral composition of the light regime along the latitudinal dimension can be discounted as a forcing function governing latitudinal succession patterns.

CHAPTER VI

SUMMARY AND CONCLUSIONS

The objective of the present study was to examine the role which division specific differences in photosynthetic action spectra play in governing the spatial and temporal distribution of the phytoplankton. In theory these differences adapt the various phytoplankton divisions to different portions of the spectral gradients in the water column. These gradients owe their origins to changes in the atmospheric light regime due to changes in solar altitude, and to the differential absorption properties of the water column. These effects should lead to changes in community composition along the vertical, latitudinal, diurnal, and seasonal dimensions.

In testing this hypothesis a numerical modeling approach has been taken. The atmospheric light regime was defined utilizing a radiative transfer model incorporating both diffuse and direct light regime components. Aerosol loading and solar altitude were the primary variables built into the model. This permitted the light regime incident on the sea surface to be defined for any time of day, latitude, or day of the year at various levels of atmospheric turbidity. The hydrospheric light regime was defined by means of an exponential decay model assuming Jerlov's (1965) Oceanic III set of attenuation coefficients, and inputs from the atmospheric model.

Given the oceanic light regime generated by the radiative transfer models the diatom and dinoflagellate carbon synthesis rates were determined at various depths by means of a spectrally sensitive photosynthetic model. Total daily carbon synthesis was determined for a unit

surface area through a finite difference summation scheme. Differences in carbon synthesis between diatoms and dinoflagellates were obtained by incorporating their respective action spectra into the photosynthetic model. This was achieved by the application of an empirical relationship defining I_k in terms of action spectrum response.

In order to examine the effect of spectral composition on community make-up the ratio between diatom and dinoflagellate carbon synthesis (ψ) was calculated along all four dimensions. It was assumed that both groups contributed the same fraction of synthesized carbon to their respective population carbon pools. Therefore, variations in ψ were viewed as reflecting differences in adaptation of the two groups at various points along a gradient.

Changes in ψ were detected along each of the four gradients considered. The largest variations (up to 22%) were detected as a function of depth and solar altitude (time of day). These variations suggested that the diatoms were best adapted for photosynthesis at relatively low sun angles (early morning and late afternoon), and with increasing depth. The converse was true of the dinoflagellates. These effects appear to be due to the enhanced photosynthetic capabilities of the diatoms over the dinoflagellates in the blue and red portions of the spectrum. (Blue light is relatively more important at increased depths, while red light is relatively more important at low sun angles.) These findings correlate with findings suggesting that the diatom populations increase with increasing depth. However, it is unlikely that the differences in ψ as a function of time of day could lead to a pattern of diurnal succession; cell division rates are far too slow for these differences to be reflected in population sizes over the course of a

single day. It may be that the diurnal changes in ψ are important in resource partitioning, acting as a temporal isolation mechanism. As such the phenomenon may be relevant in terms of Hutchinson's paradox of the plankton, helping to explain the persistence of a multispecies community despite the inevitable differences in adaptive capabilities.

Seasonal and latitudinal changes in ψ were found to be of smaller magnitude than those found along the vertical and diurnal dimensions. At equatorial latitudes ψ was essentially constant over the course of the year, indicating the absence of a seasonal pattern of succession. At temperate latitudes changes in ψ suggested that the dinoflagellates are favored during the winter months, while diatoms are favored during the summer months. This does not correlate well with the real world observation that diatoms dominate the winter community and dinoflagellates the summer community. However, this discrepancy is not considered serious. At high latitudes the fluctuations in ψ were relatively large (up to 10%) but were characterized by a seasonal shift favoring the diatoms during the winter, and the dinoflagellates during the summer. This correlates well with the real world observations of a shift from diatom to dinoflagellate community dominance with the passage from winter to summer.

Changes in ψ as a function of latitude suggest that at any given date increasing latitude favors the dinoflagellates. This is not consonant with real world observations that the diatoms are favored with increasing latitude. However, changes in ψ predicted by the model are again small (less than 3%) and the discrepancy is not considered significant.

In summary, it appears that the division specific differences in photosynthetic action spectra between diatoms and dinoflagellates are of

ecological significance. This is particularly true in terms of the vertical and diurnal gradients in spectral composition along which the changes in ψ were found to be the greatest. Changes in spectral composition appear to favor the establishment of a vertical succession from dinoflagellate to diatom dominance in the water column with increasing depth. While diurnal changes in ψ were large it is felt that they can not be relevant in establishing a diurnal succession pattern, though they may be significant in other ecological processes. Seasonal and latitudinal changes in ψ were found to be less pronounced, and therefore less important in establishing successional patterns. However, at high latitudes the seasonal changes in ψ become larger, and are consonant with the real world pattern of seasonal succession. Latitudinal patterns of succession driven by differences in light regime and action spectra are unsupported in the present study.

The model developed in the present study represents an advancement in the treatment of planktonic photosynthetic response in that it permits the consideration of spectral effects. In this instance consideration has been restricted to the examination of the role which spectral composition and division specific photosynthetic action spectra play in governing community composition. A number of other topics could be equally well explored utilizing the basic approach employed here. Some of these topics are outlined in the following paragraphs.

The hydrospheric light regime depends in part on the set of attenuation coefficients employed. These coefficients define the optical water type present in the environment. In the present study consideration has been restricted to coefficients characterizing moderately turbid oceanic conditions. Selection of other sets of attenuation

coefficients would permit consideration of photosynthetic responses under a full spectrum of marine environments ranging from highly turbid coastal conditions to extremely clear mid oceanic conditions. It would be particularly interesting to examine the effect of such manipulation on relative responses of the diatoms and dinoflagellates.

The well known Green-Brown-Red benthic macroalgal zonation pattern has been traditionally interpreted in terms of both spectral and intensity gradients. Undoubtedly both factors play a role in governing vertical distribution patterns but the relative importance of each is unclear. With appropriate modifications for benthic algal photosynthesis, and the substitution of appropriate photosynthetic action spectra the present model could be employed in resolving this problem.

The present study has shown that changes in atmospheric turbidity significantly influence both total daily carbon synthesis and community composition. It would be of interest to examine this problem in some detail. Since atmospheric turbidity varies as a function of season and latitude, its influence on carbon synthesis may have some bearing on oceanic patterns of primary production, and on seasonal and latitudinal successional patterns. Also, as figure IV-10 shows, increased turbidity depresses daily carbon synthesis to a much greater extent at high rather than at low latitudes (49% versus 19%). This implies that atmospheric pollutants of an aerosol nature can be much better tolerated at equatorial than polar latitudes. This has obvious implications for global industrialization and efforts to protect the environment.

Changes in atmospheric ozone concentrations can be induced either through nuclear warfare or the build-up of atmospheric chlorofluorocarbon compounds. Reduction of the ozine shield would result in

elevated ultraviolet radiation levels at the earth's surface. Since such radiation exerts an inhibitory effect on photosynthetic response severe consequences may be anticipated for marine primary production. This problem could readily be examined through the application of the present model by incorporating an ultraviolet-photoinhibitory function in the photosynthetic model, and extending the radiative transfer model to cover wavelengths below 300 nannometers.

REFERENCES

Allen, M.B., (Ed.), 1960. Comparative biochemistry of photoreactive systems. xii + 437.

Angstrom, A.K., 1961. Techniques of determining the turbidity of the atmosphere. Tellus 13:214-223.

Baly, E.C.C., 1934. Kinetics of photosynthesis. Nat. 134:933.

Baly, C.C, and Morgan, L.B., 1934. Kinetics of photosynthesis and allied processes. Nat. 133:414

Bannister, T.T., 1974a. Production equations in terms of chlorophyll concentration, quantum yield and the upper limit to production, Limnol. and Oceanogr. 19:1-12.

_____, 1974b. A general theory of steady state phytoplankton growth in a nutrient saturated layer. Limnol. and Oceanogr. 19:13-19.

Bennet, A., and Bogorad, L., 1973. Complementary chromatic adaptation in a filamentous blue-green alga. J. Cell. Biol. 58:419-435.

Berthold, G., 1882. Uber die Verteilung der Algen im Golf von Neapel, Mitt. Sta. Nepel 3:393-536.

Bishop, N.I., 1967. Comparison of the action spectra and quantum requirements for photosynthesis and photoreduction of Scenedesmus. Photochem, and Photobiol. 6:621-628.

Bogorov, G.G., 1958. Perspectives in the study and seasonal changes of plankton and of the number of generations at different latitudes.

Brody, M., and Emerson, R., 1959. The quantum yield of photosynthesis in Porphyridium curentum and the role of chlorophyll in the photosynthesis of red algae. J. Gen. Physiol. 43:251-264.

Brown, T.J., and Geen, G.H., 1974. The effect of light quality on carbon metabolism and extracellular release of Chlamydomonas reinhardtt II Dangered. J. Phycol. 10:213-220.

Brown, T.E., and Richardson, F.L., 1967. Development of red pigmentation in Chlorococum wimmeri (Chlorophyta:Chlorococcales). Phycol. 6:167-184.

Brown, T.E., and Richardson, F.L., 1968. The effect of growth environment on the physiology of algae: light intensity. J. Phycol. 4:38-54.

Burk and Lineweaver, 1935. Cold Springs Harb. Sym. Quant. Biol. 3:165. As cited in Rabinowitch, 1951.

Burt, W.V., 1954. Specific scattering by uniform minerogenic suspensions. Tellus 6:229-231.

Buzzat and Traverso, A.A., 1958. Perspectives in marine biology. Univ. of Calif. Press. Berkley, Calif. xvi + 621.

Calabrese, G., 1972. Research on red algal pigments 2, pigments of Petrogolssum incasenae (Duby) Schotter (Rhodophyceae, Gigartinales) and their seasonal variation at different light intensities. Phycologia. 11:141-146.

Calabrese, G., and Felicini, G.P., 1973. Research on red algal pigments. V: The effect of the intensity of white and green light on the rate of photosynthesis and its relationship to pigment composition in Gracilaria compressa (C. Ag.) Grev. (Rhodphyceae, Gigartinales). Phycologia 12:195-199.

Carreto, J.I., and Catoggio, J.A., 1971. Variations in pigment contents of the diatom Phaeodactylum tricornutum during growth. Mar. Biol. 36:105-112.

Chapman, V.J., 1957. Marine Algal Ecology. Bot. Rev. 23: 321-350.

Conover, J.T., 1958. Seasonal growth of benthic marine plants as related to environmental factors in an estuary. Univ. Texas Inst. Mar. Sci. 5:97-147.

Coulson, K.L., 1975. Solar and terrestrial radiation: methods and measurements. Academic Press, N.Y. x+ 322.

Coulson, K.L., Dave, J.V., and Sekera, Z, 1960. Tables related to radiation emerging from a planelary atmosphere with raleigh scattering. Univ. Cal., Berkley.

Crisp, D.J., 1971. The fourth European Marine Biology Symposium, Cambridge Univ. Press ix + 599.

Deirmenjan, D., and Sekera, Z., 1954. Global radiation resulting from multiple scattering in a rayleigh atmosphere. Tellus 4:382-398.

Dugdale, R.C., 1975. Biological Modeling. In: Nihoul 1975:187-205.

Dunston, W.M., 1973. A comparison of the photosynthesis-light intensity relationship in phylogenetically different marine microalgae. J. Exptl. Mar. Biol. Ecol. 13: 181-187.

Dutton, J., and Manning, W.M., 1943. Evidence for carotenoid sensitized photsynthesis in the diatom Nitzchia closterium. Am. J. Bot. 28:516-526.

Emerson, R., and Green, L., 1934. Kinetics of photosynthesis. Nat. 134:289-290.

Emerson, R., and Lewis, C.M., 1943. The dependence of quantum yield of Chlorella photosynthesis on wavelength of light. Am. J. Bot. 30:165-178.

Emerson, R., and Rabinowitch, E., 1960. Red drop and the role of auxilliary pigments in photosynthesis. Pl. Physiol. 35:477-485.

Emerson, R., Chalmers, R., and Cederstrand, C., 1957. Some factors influencing the long wave limit of photosynthesis. PNAS 43:133-143.

Englemann, T.W., 1883. Farbe and Assimilarion. Bot. Zentralbl. 41:1-29. As cited by Zaneveld, 1969.

Fee, E.J., 1969. A numerical model for the stimulation of photosynthetic production integrated over time and depth in natural waters, Limnol. and Oceanog. 14:906-11.

_____, 1973. A numerical model for determining integral primary production and its application to Lake Michigan. J. Fish. Res. Brd. Can. 30:1447-1468.

Fogg, G.E., 1975. Algal cultures and phytoplankton ecology. Univ. Wisc. Press, Madison, Wisc. xv + 175.

Forbes, E., 1844. On the connexion (sic) between the distribution of the existing fauna and flora of the British Isles, and the geological changes which have affected their area, especially during the epoch of the northern drift. London.

Fork, D.C., and Amesz, J., 1967. Slight induced shifts in the absorption spectrum of carotenoids in red and brown algae, Photoch. Photobiol. 6:621-628.

Ganf, G.G., 1975. Photosynthetic production and irradiation. Photo synthetic relationships of the phytoplankton from a shallow equatorial lake, Lake George, (Uganda). Oecologia 18:165-183.

Goldman, C.R., Mason, D.T., and Wood, J.B., 1963. Light injury and inhibition in antartic freshwater phytoplankton. Limnol. and Oceanogr. 8:313-322.

Govindjee, Rabinowitch, E., and Thomas, J.B., 1961. Inhibition of photosynthesis in certain algae by extreme red light. Biophys. J. 1:91-97.

Govindjee, Cederstrand, C., and Rabinowitch, E., 1971. Existence of absorption hands at 730-740 and 750-760 millimicrons in algae of different divisions. Sci. 143:391-392.

Guerin-Dumartrait, E., Hoaraû, J., Leclerc, J. and Sarda, C., 1975. Effets de quelques conditions d'eclairement, notamennt de la lumiere rouge, sur la compositon pigmentaire et la structure de Porphyridium sp. (Lewin). Phycologia 12:119-130.

Halldal, P., 1964. Ultraviolet action spectrum of phytosynthesis and photosynthetic inhibition in a green and a red alga. Phys. Plant. 17:414-421.

_____, 1967. Ultraviolet action spectra in algology: a review. Photoch. Photobiol. 6:445-460.

_____, 1968. Photosynthetic capacities and action spectra of endozoic algae of the massive coral Favia. Biological Bull. 137:411-424.

_____, 1969. Automatic recording of action spectra of photobiological processes, spectrophotometric analyses, fluoresence measurements and recording of the first derivitives of the absorption curve in one simple unit. Photochem. Photobiol. 10:23-34.

Hart, T.J., 1934. On the phytoplankton of the southwest Atlantic and the Bellinghouse Sea. Discovery Rept. 8:1-268. As cited by Moore, 1966.

Haxo, F.T., 1960. The wavelength dependence of photosynthesis and the role of accessory pigments, In: Allen 1960:339-360.

Haxo, F.T., and Blinks, L.R., 1950. Photosynthetic action spectra of marine algae. J. Gen. Physiol. 33:389-422.

Haxo, F.T., and Clendenning, K.A., 1953. Photosynthesis and phototaxis in Ulva lactuca gametes. Biol. Bull. 105:103-114.

Haxo, F.T., and Fork, D.C., 1959. Photosynthetically active accessory pigments of cryptomonads. Nat. 184:1051-1053.

Healy, F.P., 1972. Photosynthesis and respiration of some artic seaweeds. Phycologia 11:267-271.

Hecht, S., 1923. Sensory adaptation in the stationary state. J. Gen. Physiol. 5:555-579.

_____, 1935. A theory of visual intensity discrimination. Gen. Phys. 18:767-789.

Hitchcock, G.L., and Smayda, T.J., 1977. The importance of light in the initiation of the 1972-1973 winter-spring diatom bloom in Narragansett Bay. Limnol. and Oceanogr. 22:126-131.

Hoyt, W.D., 1920. Marine algae of Beaufort, N.C., and adjacent regions. Bull. Bur. Fish. 36:367-566 + v, pls. 84-119.

Idso, S.B., and Foster, J.M., 1975. An anlytical study of three characteristic forms of light forced primary production in aquatic exosystems. Oecologia 18:145-154.

Iverson, R.L., and Curl, H., 1973. Action spectrum of photosynthesis for Skeletonema costatum obtained as carbon-14. Phys. Plant. 28:498-502.

Jassby, A.D., and Platt, T., 1976. Mathematical formulations of the relationship between photosynthesis and light for phytoplankton. Limnol. and Oceanog. 21:540-547.

Jerlov, N.G., 1968. Optical oceanography. Elsevier Publ. Co., Amsterdam. xiii + 194.

Johnson, D.S., and Skutch, A.T., 1928a. Littoral vegetation on a headland of Mt. Desert Island, Maine. I. submersible and strictly littoral vegetation. Ecol. 9:188-215.

_____, 1928b. Littoral vegetation on a headland of Mt. Desert Island, Maine. II. Tide pools and the environment and classification of submersible plant communities. Ecol. 9:307-338.

Jones, L.W., and Myers, J., 1965. Pigment variation in Anacystis nidulans induced by light of selected wavelengths. J. Phycol. 1:6-13.

Jorgensen, E.G., 1969. The adaptation of planktonic algae. IV Light adaptation in different algal species. Physiol. Plant. 22:1307-1315.

Kain, J.M., 1971. Continuous recordings of underwater light in relation to Laminaria distribution. In: Crisp 1971:335-346.

Kain, J.M., and Fogg, G.E., 1958a. Studies on the growth of marine phytoplankton I. Asterionella japonica Gran. JMBAUK 37:397-413.

_____, 1958b. Studies on the growth of marine phytoplankton. II. Isochrysis galbana Parke. JMBAUK 37:781-788.

_____, 1960. Studies on the growth of marine phytoplankton III. Procentrum micans Ehrenberg. JMBAUK 39:33-50.

Kiefer, D., and Strickland, J.D.H., 1970. A comparative study of photosynthesis in seawater samples incubated under two types of light attenuator. Limnol. and Oceanogr. 15:408-412.

Kimball, H.H., 1924. Records of total solar radiation intensity and their relation to daylight intensity. Monthly Weather Rev. 52:573-479.

Kirk, J.T.O., and Reade, J.A., 1970. The action spectrum of photosynthesis in Euglena gracilis at different stages of chloroplast development. Aust. J. Biol. Sci. 23:33-41.

Kok, B., 1956. On the inhibition of photosynthesis by intense light. Bioch. and Biophys. Acta. 21:234-244.

Lazaroff, N., 1966. Photoinduction and photoreversal of the Nostocacean development cycle. J. Phycol. 2:7-17.

Lehman, J.T., Botkin, D.B., and Likens, G.E., 1975. The assumptions and rationales of a computer model of phytoplankton population dynamics. Limnol. and Oceanogr. 20:343-364.

Levring, T., 1960. Submarines Licht und die Algenyegetation. Bot. Mar. 1:67-73.

Lewis, W.M., 1974. Primary production in the phytoplankton community of a tropical lake. Ecol. Monogr. 44:377-409.

Lipps, M.J., 1973. The determination of the far-red effect in marine phytoplankton. J. Phycol. 9:227-242.

Luning, K., 1971. Seasonal growth of Laminaria hyperborea under recorded underwater light conditions near Helgoland, In: Crisp 1971: 347-361.

MacIsaac, J.J., 1978. Diel cycles of inorganic nitrogen uptake in a natural phytoplankton population dominated by Gonyaulax polyedra. Limnol. and Oceanogr. 23:1-9.

Mandelli, E.F., 1972. The effect of growth illumination on the pigmentation of a marine dinoflagellate. J. Phycol. 8:367-369.

Mann, J.E., and Myers, J., 1968. On pigments growth and phytosynthesis of Phaeodactylum tricornutum. J. Phycol. 4:349-355.

_____, 1968. Photosynthesis enhancement in the Diatom Phaeodactylum tricornutum. Pl. Physiol. 43:1991-1995.

Margalef, R., 1958. Temporal succession and spatial heterogeneity in phytoplankton. In: Buzzati:-Traverso 1958:323-349.

Margulies, M.M., 1970. Changes in absorbance spectrum of the diatom Phaeodactylum tricornutum upon modification of protein structure. J. Phycol. 6:160-164.

Martin, J.H., 1970. Phytoplankton-zooplankton relationships in Narragansett Bay. 4. The seasonal importance of grazing. Limnol. and Oceanogr. 15:413-418.

McCulough, E.C., and Porter, W.P., 1971. Computing clear day solar radiation spectrum for the terrestrial ecological environment. Ecol. 52: 1008-1015.

McCleod, G.C., 1961. Action spectra of light saturated photosynthesis. Pl. Physiol. 36:114-117.

McCleod, G.C., and Kanwisher, J., 1962. Quantum efficiency of action spectrum in ultraviolet light. Physiol. Plant. 15:581-586.

Moore, Hillary B., 1966. Marine Ecology. John Wiley and Sons, Inc. New York. 493 + xi.

Morel, A., and Smith, R.C., 1974. Relation between total quanta and total energy for aquatic photosynthesis. Limnol. and Oceanogr. 19:591-600.

Myers, J., and Kratz, W., 1955. Relations between pigment content and photosynthesis characters in a blue-gree alga. J. Gen. Physiol. 39:11-22.

Myers, J., and Burr, G.O., 1941. Studies on photosynthesis: some effects of light of high intensity on Chlorella. J. Gen. Phys. 24:45-67.

Nagel, M.R., 1974. An improved approximation of Bemporad's air mass function. Appl. Optics 13: 1008-1009.

Nassau, J.J., 1948. Practical Astronomy. McGraw Hill, N.Y. xi:+311.

Nihoul, T.C.J., 1975. Modeling of marine systems. Elsevier Science Publ. Co., Amsterdam. xix - 272.

O'Brien, W.S., 1974. The dynamics of nutrient limitation of phoyoplankton algae: A model reconsidered. Ecol. 55:135-141

Oersted, A.S., 1844. De Regionibus Marinis Elementa topographiae historia naturalis freti Oersund. Copenhagen.

Ofelt, G.S., 1976. Relation between beam and diffuse attenuation coefficients in the lower Chesapeake Bay area. Technical Report 32. Inst. Oceanography, Old Cominion University, Norfolk, Va. ii - 17.

Oltmanns, F., 1892. Uber die Kulture- und Lebendingungen der Meersalgen. Jahrb. Wiss. Bot. 23.

O'Quist, G., 1969. Adaptations in pigment composition and photosynthesis by far-red radiation in Chlorella pyrenoidosa. Phys. Plant. 22:516-528.

Paasche, E., 1966. Action spectrum of coccolith formation. Phys. Plant. 17:770-779.

Parsons, T.R., and Takahashi, M., 1974. Biological oceanographic processes. Pergamon Press, N.Y.

Patrick, R., Crum, B., and Coles, J., 1969. Temperature and manganese as determining factors in the presence of diatom of blue-green algal floras in streams. PNAS 64:472.

Patten, B.C., 1968. Mathematical models of plankton production. Int. Rev. Gesamten Hydrobiol. 53:357-408.

Pickett, J.M., and Myers, J., 1966. Monochromatic light saturation curves for photosynthesis in Chlorella. Plant. Physiol. 41:90-09.

Plass, G.N., and Kattawar, G.W., 1968. Monte Carlo calculations of light scattering from clouds. Appl. Optics 7:415-419.

_____, 1969. Radiative transfer in the Atmosphere-Ocean system. Appl. Optics. 8:455-466.

_____, 1972. Effects of aerosol variation on radiance in the earth's atmosphere-ocean system. Appl. Optics. 11:1598-1604.

_____, 1972. Monte Carlo calculations of radiative transfer in the earth's atmosphere and ocean systems. I: Flux in the atmosphere and ocean. J. Phys. Oc. 2:136-145.

Plass, G.N., Kattawar, G.W., and Catchngs, F.E., 1973. Matrix operator theory of radiative transfer. 1. Rayleigh scattering. Applied Optics. 12:314-329.

Platt, T., and Jassby, A.D., 1976. The relationship between photosynthesis and light for natural assemblages of coastal marine phytoplankton. J. Phycol. 12:421-430.

Pratt, D.M., 1965. The winter-spring diatom flowering in Narragansett Bay. Limnol. and Oceanogr. 10:173-184.

Qasim, S.Z., Bhattathiri, P.M.A., and DeVassy, U.P., 1972. The effect of intensity and quality of illumination on the photosynthesis of some tropical marine phytoplankton. Mar. Biol. 16:22-27.

Quaraishi, F.O., and Spencer, C.P., 1971. Studies on the response of marine phytoplankton to light fields of varying intensity. In: Crisp 1971. 393-408.

_____, 1971. Studies on the growth of some marine unicellular algae under different light sources. Mar. Biol. 8:60-65.

Rabinowitch, E.I., 1951. Photosynthesis II(1). Interscience Publ. Inc., N.Y. xi + 603-1208.

Rabinowitch, E., Govindjee, and Thomas, J.B., 1960. Inhibition of photosynthesis in some algae by extreme red light. Sci. 132:422.

Raymont, J.E.G., 1963. Plankton and productivity in the oceans. MacMillan, New York. viii-660.

Riley, G.A., 1957. Phytoplankton in the north central Sargasso Sea 1950-52. Limnol. and Oceanogr. 2:252-270.

Rodhe, W., Vollenweider, R.A., and Nauwerk, A., 1958. The primary production standing crop of phytoplankton. In: Buzzati:-Traverso 1958:299-322.

Rozenberg, E.V., 1966. Twilight: A study in atmospheric optics. Plenum Press. Reprint of 1963 Russian edition. x + 358.

Ryther, J.H., 1956. Photosynthesis in the ocean as function of light intensity. Limnol. and Oceanogr. 1:61-70.

Sekera, Z., and Kahle, A.B., 1966. Scattering functions for Rayleigh atmospheres of arbitrary thickness. Rep. No. R-452-PR. The Rand Corp., Santa Monica, Calif. 1-73.

Setchell, W.A., 1920. The temperature interval in the geographic distribution of marine algae. Sci. 42(1339):187-190.

Shannon, J.G., 1975. Correlation of beam and diffuse attenuation coefficients measured in selected ocean waters. SPIE 64:3-10.

Smayda, T.J., 1957. Phytoplankton studies in lower Narragansett Bay. Limnol. and Oceanogr. 2:342-359.

_____, 1973. The growth of Skeletonema costatum during a winter-spring bloom in Narragansett Bay, Rhode Island. Norw. J. Bot. 20:219-247.

Swift, L.W., 1976. Algorithm for solar radiation on mountain slopes. Water Resources Research 12:108-112.

Smith, E.I., 1936. Photosynthesis in relation to light and carbon dioxide. PNAS 22:504-510.

_____, 1937. The influence of light and carbon dioxide on photosynthesis. J. Gen. Physiol. 20:807-830.

_____, 1939. Limiting factors in photosynthesis: light and carbon dioxide. J. Gen. Physiol. 22:21-35.

Sorokin, C., and Krauss, R.W., 1958. The effects of light intensity on the growth of green algae. Pl. Phys. 33:109-113.

Steele, J.H., 1962. Environmental control of photosynthesis in the sea. Limnol. and Oceanogr. 7:137-150.

Steele, J.H., and Menzel, D.W., 1964. Conditions for maximum primary production in the mixed layer. Deep Sea Research 9:39-49.

Steeman-Nielsen, E., 1962. Inactivation of the photochemical mechanism in photosynthesis as a means to protect the cells against high light intensity. Physiol. Plant. 15:161-171.

_____, 1975. Marine photosynthesis with special emphasis on the ecological aspects. Elsevier Sci. Publi. Co., Elsevier Oce. Ser. 13, Amsterdam. ix + 141.

Talling, J.F., 1957a. Photosynthetic characteristics of some fresh-water phytoplankton diatoms in relationship to underwater radiation. New Phytol. 56:29-50.

_____, 1957b. The phytoplankton population as a compound photosynthetic system. New Phytol. 56:133-149.

Tanada, T., 1951. The photosynthetic effect of carotenoid pigments in Navicula minima. Am. J. Bot. 38:276-283.

Thekera, M.P., and Drummond, A.J., 1971. Standard values for the solar constant and its spectral components. Nat. Phys. 229:6-9. (Corregium Nat. Phys. 229:244.)

Twomey, S., Jacobowitz, H., and Howell, H.B., 1966. Matrix methods for multiple-scattering problems. J. Atmos. Sci. 23:289-296.

Vollenweider, R.A., 1965. Calculation models of photosynthesis-depth curves and some implications regarding day rate estimates in primary production measurements. IN: Goldman 1966:425-457.

Von Gaidukov, N., 1904. Zur Farben analyse de Algen. Ber. Deut. Bot. Gessel. 22:23.

_____, 1904. Ber. Deut. Bot. Ges. 22:23. As cited by Zaneveld, 1969.

Waaland, J.R., Waaland, S.D., and Bates, G., 1974. Chloroplast structure and pigment composition in the red alga Griffithsia pacifica: regulation by light intensity. J. Phycol. 10:193-199.

Wallen, D.G., and Geen, G.H., 1971a. Light quality in relation to growth, photosynthetic rates, and carbon metabolism in two species of marine plankton algae. Mar. Biol. 10:34-43.

_____, 1971b. Light quality and concentration of proteins, RNA, DNA, and photosynthetic pigments in two species of marine plankton algae. Mar. Biol. 10:44-54.

_____, 1971c. The nature of the photosynthate in natural phytoplankton populations in relation to light quality. Mar. Biol. 10:157-168.

Wassink, E.C., and Kersten, J.A.H., 1946. Observations seur le spectre d'absorption et sur le role des carotenoides dans in photosynthese des diatomees. Enzymologia 12:3-32.

Williams, L,G., 1948. Seasonal alternation of marine floras at Cape Lookout, North Carolina. Am. J. Bot. 35:682-695.

Winter, D.F., Banse, K., and Anderson, G.C., 1975. The dynamics of phytoplankton blooms in Puget Sound, a fjord in the northwestern United States. Marine Biol. 29:139-176.

Yocum, C.S., and Blinks, C.R., 1954. Photosynthetic efficiency of marine plants. J. Gen. Physiol. 38:116.

Zaneveld, J.S., 1969. Factors controlling the elevation of littoral benthic marine algae. Amer. Zool. 9:367-391.

AUTOBIOGRAPHICAL STATEMENT

William Morrow Willis was born 19 October 1944, in Baltimore, Maryland. His parents are Thurston L. Willis and Evelyn F. Morrow. As a youth he lived in the states of Washington (Seattle and southwestern regions), California (Long Beach), New Jersey (Cape May), and Virginia (Portsmouth). He received a B.S. degree in Biology from the College of William and Mary in 1967. In 1973 he received an M.S. degree in Oceanography from Old Dominion University. He married Brenda Louise Marshall on 17 June 1972. Their first child is expected in September 1978.

Mr. Willis was employed for five years as a teacher in the Virginia school systems, first (1967-1968) with Chesapeake City Schools, and later (1968-1970, 1972-1975) with Portsmouth City Schools. At Old Dominion University he held research assistantships during the periods 1970-1971, and 1976. He is currently employed as a marine ecologist with Science Applications, Inc., a research consulting firm centered in La Jolla, California. His present address is 800 Oak Ridge Turnpike, Oak Ridge, Tennessee 37830.